3-10-2010

Optical Properties of Si, Ge, GaAs, GaSb, InAs, and InP at Elevated Temperatures

Thomas R. Harris

OPTICAL PROPERTIES OF SI, GE, GAAS, GASB, INAS, AND INP AT ELEVATED TEMPERATURES

THESIS

Thomas R. Harris

AFIT/GAP/ENP/10-M08

DEPARTMENT OF THE AIR FORCE
AIR UNIVERSITY

AIR FORCE INSTITUTE OF TECHNOLOGY

Wright-Patterson Air Force Base, Ohio

The views expressed in this thesis are those of the author and do not reflect the official policy or position of the United States Air Force, Department of Defense, or the United States Government.

AFIT/GAP/ENP/10-M08

OPTICAL PROPERTIES OF SI, GE, GAAS, GASB, INAS, AND INP AT ELEVATED TEMPERATURES

THESIS

Presented to the Faculty

Department of Engineering Physics

Graduate School of Engineering and Management

Air Force Institute of Technology

Air University

Air Education and Training Command

In Partial Fulfillment of the Requirements for the

Degree of Master of Science in Engineering Physics

Thomas R. Harris, BS

DAGSI

March 2010

AFIT/GAP/ENP/10-M08

OPTICAL PROPERTIES OF SI, GE, GAAS, GASB, INAS, AND INP AT ELEVATED TEMPERATURES

Thomas R. Harris

DAGSI

Approved:

_____	_____
Yung Kee Yeo, PhD (Chairman)	Date
_____	_____
Shekhar Guha, PhD (Member)	Date
_____	_____
Robert Hengehold, PhD (Member)	Date

Abstract

Investigation of the optical and electrical behavior of some semiconductors at very high temperatures has not been an area of much study, at least not experimentally. The importance of such research becomes obvious due to the effects of high temperatures on semiconductor devices such as infrared detectors and light emitters. Besides the destructive effects of thermal stress and melting, changes in the optical properties of the material can greatly affect device performance. In this research, the infrared absorption of Si, Ge, GaAs, GaSb, InAs, and InP was measured from 0.6 to 25 μm at temperatures ranging from 295 up to 900 K, using a Fourier Transform InfraRed (FTIR) spectrometer in combination with a custom-designed heater assembly. The band gap shift was estimated from the experimental results and compared to existing data. There was good agreement between the two results. For GaSb and InAs, data was taken at higher temperatures than what was found in the literature. That data provides an extension of existing theory to a higher temperature range. Free-carrier absorption was also observed and was compared to existing data. Temperature dependent expressions were developed for the band gap energy and free-carrier absorption in Si, Ge, GaAs, GaSb, InAs, and InP.

Acknowledgments

First of all I would like to thank Drs. Yeo and Guha, my AFIT and AFRL advisors. Their help and guidance was crucial to the success of this work. To the other folks at AFRL: thanks to Dr. Leo Gonzales for his assistance. Thanks to Derek Upchurch and Jacob Barnes for their help in the lab and to Jack Barnes for his work in designing the heater and related parts. Thanks to Amelia Carpenter for showing me how to use the spectrometer and for emailing me all of my data files because I didn't have an external hard drive. To those at AFIT: Thanks to Greg Smith for his help in sample preparation and just general advice. Thanks to Rick Patton and Rich Johnston for providing clean room training and services. Thanks to Dr. Woo Jun Yoon for his insight and helpful advice. The last category of people to whom I owe thanks is my family. Though their help was not technical or scientific, it was nonetheless invaluable. To my parents, you are the reason I am where I am today. Thank you for your love and support, both moral and financial, through the years. To my in-laws, thank you for the friendly reminders and encouraging words, they really meant a lot. Lastly, to my wife, I could never have done this without your constant love and support. For putting up with all the late nights, and an often frustrated and grumpy husband, thank you.

Thomas Harris

Table of Contents

List of Figures

Figure Page

Figure Page

List of Tables

OPTICAL PROPERTIES OF SI, GE, GAAS, GASB, INAS, AND INP

AT ELEVATED TEMPERATURES

I. Introduction

Background

The infrared absorption of semiconductors has been a topic of research for almost as long as the topic of semiconductors itself. Materials like Si and Ge have been studied extensively starting in the 1950's and are currently used in a myriad of solid state devices. GaAs, InAs, InP, and GaSb lay claim to volumes of research of their own, and have been used in light emitting and optoelectronic devices. Historically the need to characterize these materials became important as growth techniques were developed and advanced. Interest in a material for a particular application also motivated research to characterize the semiconductor.

In most cases, the emphasis of the research at the time was on the fundamental physical processes underlying the observed optical behavior (in this case absorption.) As a consequence, materials were studied at temperatures ranging from very low temperatures (liquid helium, 4.2 K, or liquid nitrogen, 77 K) to about room temperature, 298 K. The reason for this was that as temperature increases, many of the finer absorption features are "drowned out" by thermal noise. The width of optical transition peaks increase with temperature and neighboring peaks blend into one another, making it

difficult to nail down the exact peak energies of the optical transitions. Because of this effect, low temperatures provided a distinct advantage in semiconductor characterization.

Objectives

The purpose of this study was to characterize the optical absorption properties of various semiconductors such as Si, Ge, GaAs, etc, and to investigate how the current knowledge applied in the limit of very high temperatures. The application of interest was essentially the effect of high temperatures on optical devices, and so the research was performed with that application in mind. More specifically, it was of interest to know at what temperature a certain semiconductor sample would become opaque, i.e. completely absorbing for that particular thickness. This would apply to semiconductors used as windows or other optical elements as well as those used in light emitters or detectors.

Semiconductor Fundamentals

The following section gives a brief introduction to solid state physics. A basic understanding of these principles is necessary in order to proceed. This section will provide a theoretical basis for the resulting discussion. Also, terms that are introduced or defined here will be used throughout the following sections. This introduction is not meant to be exhaustive. For more detail about the topics in this section, a solid state physics textbook, e.g. those by Kittel [1] or Ashcroft and Mermin [2], should be referenced.

In general, there are two classes of solids, crystalline and amorphous. Crystalline solids have a rigid crystal lattice which defines the positions of the atoms relative to one

another. Amorphous solids do not have this definite arrangement of atoms. There is no "long-range" order. For this paper, we will focus on crystalline solids since all of the samples studied were of that class. One simple way to think about the structure of a semiconductor is in two parts: 1. the rigid lattice made up of ion cores, and 2. the valence electrons. The electrons moving through the lattice see the ion cores as a "periodic potential". Using the Kroenig-Penney model for the periodic potential along with the tight binding approximation one can apply boundary conditions, and obtain solutions for the energy of the electron in terms of its wavevector k. This expression for energy in terms of k, or momentum, defines the dispersion relation for the electron.

An interesting result is that there are only valid solutions for certain ranges of energy values. The electron is no longer "free" as it is in the free electron model which works quite well at predicting the behavior of metals. These allowed energies are most often called "bands" while the disallowed energy range in between is a "band-gap". For semiconductors, there is a gap between the highest occupied band and the lowest unoccupied band (at T=0). This is what is referred to as the "band-gap" or "electronic band-gap" of the material.

Band structure diagrams are often used to show these allowed electron states. Plotted on the x-axis is k (wavevector, or momentum) and on the y-axis is energy. Full band structure calculations have been done for most materials using a pseudo-potential method. Band structure is an important topic, but for the most part, the details of such derivations will not be included in this work. The results however will be included since they are useful in visualizing the bands and various transitions for the semiconductors

studied. For examples, the band structure of Si is shown in Figure 1, and that of GaAs in Figure 2.

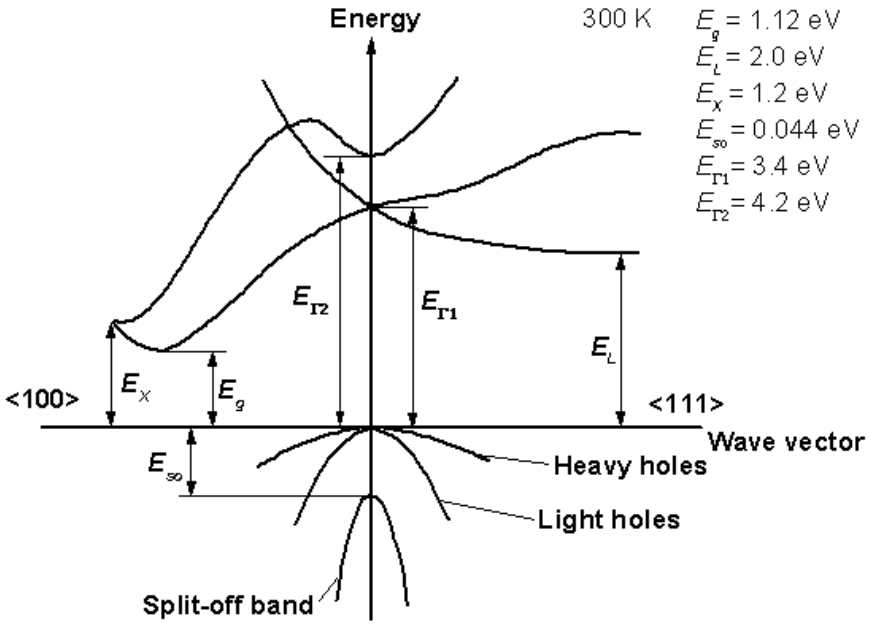

Figure 1. Band structure and parameters of Si at 300 K

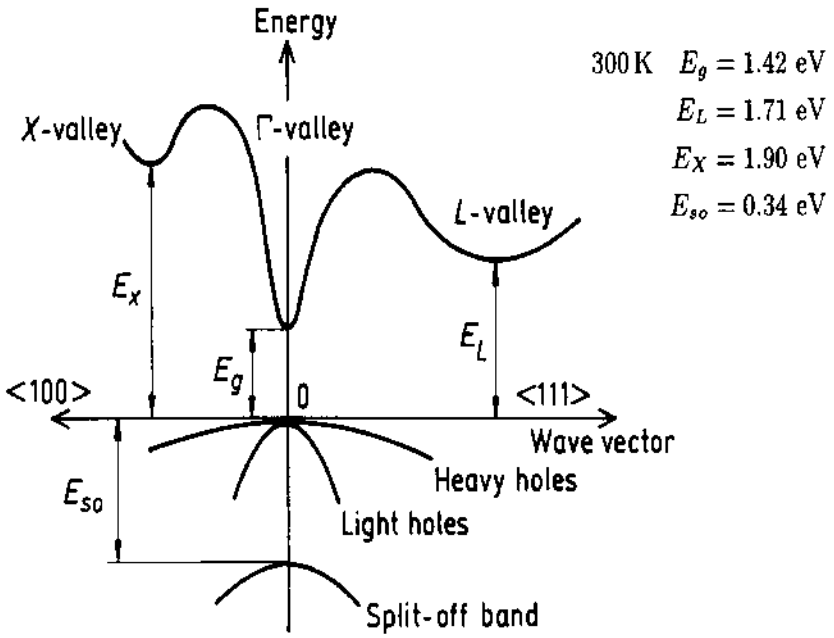

Figure 2. Band structure and energy parameters of GaAs at 300 K

The point in the band structure with the lowest energy difference is what has been defined as the band gap of the material. For Si, it can be seen from the diagram that this location (the bottom of the conduction band) does not lie directly over the top of the valence band. For this reason, it is referred to as an indirect band gap, and Si, an indirect band gap material. In order for the electronic transition to occur, it must be coupled with a phonon which imparts the electron with the momentum needed to reach the state in the conduction band. More detail on those transitions will be discussed in the section on optical properties. Other indirect band gap materials include Ge, and GaP.

In addition to indirect band gap materials, there are also of course direct band gap materials, which include GaAs, GaSb, InAs, and InP among others. In these cases the electron may be excited without the assistance of a phonon and can be seen as a more abrupt absorption edge in the spectra. Different materials are also classified by the magnitude of their band gap energy into one of three categories: narrow-bandgap, mid-bandgap, and wide-bandgap. A scatter plot of some common semiconductor materials versus their lattice parameter and band gap energy (or wavelength) is shown in Figure 3. The materials studied in this work are highlighted.

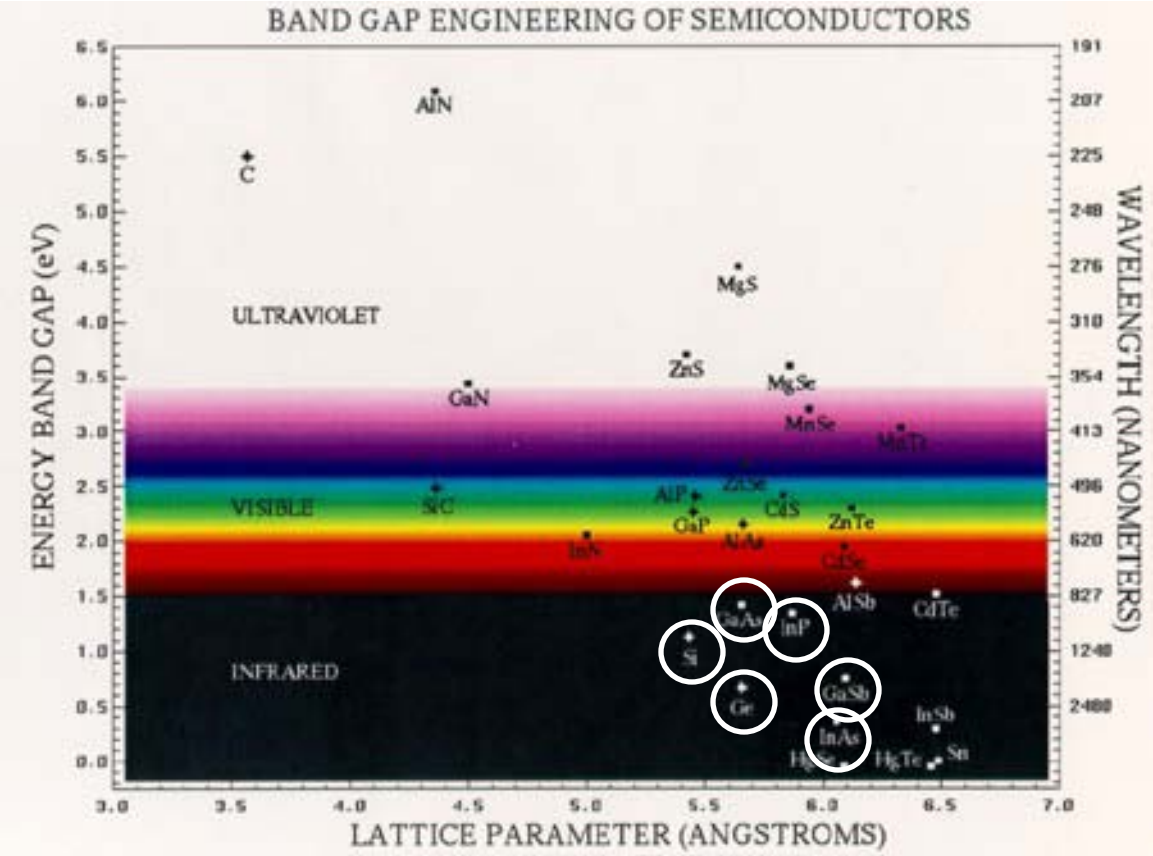

Figure 3. Band gaps of common semiconductor materials plotted as a function of their lattice parameter

Optical Characterization Theory

The interaction of light with matter can be viewed macroscopically as being comprised of four components: an incident, a reflected, a transmitted, and an absorbed (or scattered) component. The reflectance can be defined in terms of the index of refraction of the media on either side of the interface. If the index of refraction of the material is *n* and the material is surrounded by air ($n_{air} \approx 1$), then the reflectance for near normal incidence can be written as,

$$R = \left|\frac{n-1}{n+1}\right|^2.$$

The derivation of this equation can be accomplished using the laws of electricity and magnetism and by applying boundary conditions at the interface. The equations for the reflection and transmission coefficients for both states of polarization (parallel or perpendicular relative to the plane of incidence) are referred to as Fresnel's equations. The full development of those equations can be found in most graduate level E&M or Optics texts.

The absorption coefficient is defined as the fraction of the intensity absorbed per unit length in the media, i.e.

$$\alpha = -\frac{1}{I(z)}\frac{dI}{dz}.$$

This can be integrated to obtain Beer's Law

$$I(z) = I_0 e^{-\alpha z},$$

where I_0 is the intensity at the incident surface, i.e. z=0.

Another term that is associated with attenuation is what's called the optical density, or O.D. It is defined as the negative log of the ratio of the transmitted intensity, I_{out}, to the incident intensity, I_{in}, i.e.

$$O.D. = -\log_{10}\left(\frac{I_{out}}{I_{in}}\right).$$

For example, if the incident intensity was 100 mW/cm^2 and the transmitted intensity was 0.1 mW/cm^2, then the ratio $\frac{I_{out}}{I_{in}}$ would be $\frac{0.1}{100} = \frac{1/10}{100} = \frac{1}{1000} = 10^{-3}$. The optical

density, then, would be $O.D. = -\log_{10}(10^{-3}) = -(-3)(1) = 3$. So the optical density describes how many orders of magnitude the intensity has decreased after propagating through the material.

To develop our equations for transmission and reflection, let's look at a case where there is no absorption. Assuming normal incidence and that the reflectance at the two interfaces is equal, the transmitted intensity can be expressed as a function of the incident intensity as

$$I_t = (1-R)^2 I_0.$$

The squared dependence comes from the fact that there are two interfaces at which reflection occurs. The transmission coefficient or transmittance is simply the ratio of the transmitted over the incident intensity and can be written as,

$$T = \frac{I_t}{I_0} = (1-R)^2.$$

If multiple internal reflections are accounted for, the transmission becomes

$$T = \frac{(1-R)^2}{1-R^2}.$$

When absorption is added, we obtain the final form for the transmission

$$T = \frac{(1-R)^2 e^{-\alpha t}}{1-R^2 e^{-2\alpha t}}.$$

where α is the absorption coefficient and *t* is the sample thickness.

Since R depends on the refractive index and the refractive index depends on the wavelength (often called dispersion), it can be seen that the reflectance is now a function of wavelength. Since the transmission is also a function of wavelength, solving this equation will give the absorption coefficient α as a function of λ. To investigate the functional form of the transmission further, a new expression for the reflectance, R, must be obtained. In general, the refractive index (or dielectric constant) of a material can be complex, so our expressions for the reflectance and transmittance will change. If we define our complex index of refraction as

$$\tilde{n} = n + i\kappa,$$

where κ is referred to as the extinction coefficient and can be related to the absorption coefficient α by,

$$\kappa = \frac{\alpha\lambda}{4\pi},$$

where λ is the wavelength of the incident light.

Substituting these in to our expression for the reflectance, we obtain

$$R = \left|\frac{\tilde{n}-1}{\tilde{n}+1}\right|^2 = \frac{(n-1)^2-\kappa^2}{(n+1)^2-\kappa^2}.$$

Further, we can substitute in our expression for κ in terms of α to obtain R as a function of n, α, and λ. R then becomes,

$$R = \frac{(n-1)^2-\left(\frac{\alpha\lambda}{4\pi}\right)^2}{(n+1)^2-\left(\frac{\alpha\lambda}{4\pi}\right)^2}.$$

Substituting this new expression back into our equation for transmission, we get

$$T = \frac{\left[1 - \frac{(n-1)^2 - \left(\frac{\alpha\lambda}{4\pi}\right)^2}{(n+1)^2 - \left(\frac{\alpha\lambda}{4\pi}\right)^2}\right]^2 e^{-\alpha t}}{1 - \left[\frac{(n-1)^2 - \left(\frac{\alpha\lambda}{4\pi}\right)^2}{(n+1)^2 - \left(\frac{\alpha\lambda}{4\pi}\right)^2}\right]^2 e^{-2\alpha t}}.$$

Simplifying, this becomes,

$$T(\alpha, \lambda, n, t) = \frac{4096 e^{t\alpha} n^2 \pi^4}{-[16(-1+n)^2\pi^2 + \alpha^2\lambda^2]^2 + e^{2t\alpha}[16(1+n)^2\pi^2 + \alpha^2\lambda^2]^2}.$$

Solving this equation is not trivial. Because of the exponential functions, this expression cannot be solved analytically to obtain an expression for α in terms of the other variables. However, it can be solved numerically, and so an algorithm was developed to solve the equation for each value of *T* and λ obtained from the spectrometer. The values of the thickness, *t* were measured for each sample.

A simplification can be made to the previous expression for transmission if the wavelengths of interest are considered. For most infrared wavelengths, λ is of the order of $1x10^{-6}$ m. So for $\alpha < 1x10^{6}$ m^{-1} or $1x10^{4}$ cm^{-1}, the product α λ will be small, or at worst about 1. If $(\alpha\,\lambda) < 1$, then $(\alpha\,\lambda)^2 << 1$, and the expression for T becomes:

$$\frac{16 e^{t\alpha} n^2}{-(-1+n)^4 + e^{2t\alpha}(1+n)^4}$$

Or, more simply, one can compute the reflectance first, i.e. $R = \frac{(n-1)^2}{(n+1)^2}$, and then solve for the absorption using the transmission equation, i.e. $T = \frac{(1-R)^2 e^{-\alpha t}}{1-R^2 e^{-2\alpha t}}$.

Recalling our assumption, the simplification should hold as long as $\alpha < 1 \times 10^4$ cm^{-1}. As an example, consider GaAs, with an infrared refractive index, n, of 3.3, and a thickness of 0.5 mm (5×10^{-2}cm). Assume a maximum α of 100 cm^{-1} (1×10^2 is still 2 orders of magnitude less than our limit of 1×10^4). Using the above expression, this gives a transmission of 0.3434 %. For α = 1000 cm^{-1} the transmission decreases to 9.83E-21, much too low for a spectrometer to detect (see next section for discussion of maximum O.D.). So for sample thicknesses on the order of millimeters (or 1/10 of a millimeter), the maximum absorption measured would be, at most, on the order of 1E3 cm^{-1}. So our approximation should be valid in most cases.

One more effect to consider is the wavelength and temperature dependence of the refractive index. In general, the refractive index may have two types of wavelength dependence (also called dispersion), normal and anomalous. In the infrared region of interest for these materials, the dispersion is entirely normal. The variation in the refractive index in this infrared region is relatively small. For these reasons, a standard value for the infrared refractive index was used in the calculations. This approximation greatly increased the speed of the calculations since *n* was now a constant and not a function of λ. The refractive index does change with temperature so that now $n = n(T)$.

This was modeled assuming a linear relation of n and T, i.e.

$$n = n_{0K} + \left(\frac{\partial n}{\partial T}\right) T.$$

A value for $\frac{\partial n}{\partial T}$ was obtained for the materials from a handbook of optical constants. Now, finally, since the values of n(T), λ, T and t were all known, the absorption coefficient α could be calculated as a function of wavelength. Since measurements were taken at various temperatures, a temperature dependence could also be calculated so that α was now a function of both wavelength and temperature.

Absorption has been discussed briefly from a macroscopic view, but now it will be explored in more detail, especially in how it relates to semiconductor materials. There are many different types of absorption in semiconductors, or said another way, there are many processes by which a photon may be absorbed. The first, and probably the most noticeable from an experimental standpoint, is what is referred to as interband absorption. Recall our earlier discussion of "bands" and the "band-gap". Interband absorption is when an electron in the valence band absorbs a photon and is excited up into the conduction band. For a direct band gap semiconductor, the electron only increases its energy, and its momentum is unchanged. For an indirect gap material, however, the momentum is shifted. This is accomplished by either absorbing or emitting a phonon.

Interband absorption is usually the dominant process observed in infrared specta since such a large number of photons with energy above the band-gap energy are absorbed. The onset of this transition is known as the "absorption edge". It may also be referred to as a cut-on or cut-off wavelength depending on the application. For indirect

gap materials, because a phonon can be emitted or absorbed, there are multiple photon energies that can contribute to the interband absorption. So, there is some absorption for values of photon energy below the bandgap energy. This appears in the absorption spectrum as a "tail" on the absorption edge and is referred to as the "Urbach tail". This effect is clearly seen in the data for silicon and germanium which were the two indirect band gap materials studied.

The band gap decreases in energy, or shrinks, as temperature increases. This is due to two factors: thermal expansion and lattice vibrations, i.e. phonons. Thermal expansion causes the lattice constant to increase, which causes a change in the periodic potential that the electron sees. This change in potential changes the band structure and thereby changes the band gap. This band gap shift has been measured using many different methods including photoluminescence, absorption spectroscopy, wavelength modulated spectroscopy, and spectroscopic ellipsometry.

The first empirical relation for the band gap shift with temperature (besides a simple linear relation) was developed by Varshni[3], and takes the form:

$$E_g = E_g(0) - \frac{\alpha T^2}{(T+\beta)},$$

where E_g is the band gap energy and T is temperature.

$E_g(0)$ is the band gap at 0 K and has units of energy, α has units of energy/temperature (not to be confused with the absorption coefficient, also denoted by α), and β has units of temperature. β should be closely related to the Debye temperature of the material.

The Varshni expression was an empirical fit to band gap measurements taken by others in previous work, but did provide a good fit to the data. The two characteristics of the equation that accomplish that are: 1. a "leveling off" or quadratic dependence that occurs at low temperatures and 2. a linear decrease in the bandgap at high temperatures. While Varshni provided a good fit to the data at the time, it was empirical and did not have a basis in theory. Also, as more research was done, data taken seemed to suggest a slightly different temperature dependence. For those reasons, an expression was developed by L. Vina et. al. [4] which has the following form:

$$E(T) = E_B - a_B \left[1 + \frac{2}{e^{\Theta/T} - 1}\right].$$

Here, $E_B - a_B$ gives the zero temperature band gap. Both E_B and a_B have units of energy (the first in eV and the latter in meV). Θ is the phonon energy associated with the band gap shift and has units of temperature. This expression has a basis in the Bose-Einstein statistics that govern phonon occupations. For this reason, it gives a better fit to the lattice component of the band gap shift.

Assumptions and Limitations

Transmission measurements are limited, because, at a certain point, the sample will be completely absorbing. In other words, for that thickness, there is not enough light getting through the sample for the spectrometer to make a measurement. This limit is often defined as a maximum optical density (O.D.) and is usually given for the spectrometer as a rating. A typical value for the maximum O.D. is 3. In terms of

transmittance, that equates to a value of $1x10^{-3}$, or $1x10^{-1}$%=0.1% transmission. The instrument may give lower values of transmission, but the uncertainty of those values would be very large, making it difficult to use the data reliably. To find the maximum absorption the spectrometer can measure from this maximum O.D., recall the example given of GaAs. With a room temperature refractive index of 3.3, the reflectance is 0.2861. The equation for transmission defined earlier can then be solved for α to give a maximum absorption coefficient.

Assuming a thickness of 0.5 mm, and a minimum transmittance of $1x10^{-3}$, the equation gives a maximum α of $1.3x10^{4}$ m^{-1} or $1.3x10^{2}$ cm^{-1} which is 2 orders of magnitude less than 10^{4} cm^{-1}. This supports the earlier conclusion that, for infrared wavelengths, the product ($\alpha \lambda$) is small and the simplification made to the transmission equation can be used. Not only can the previous approximation be used, but a maximum absorption was found to be on the order of 100 cm^{-1} and can be assumed for most of the samples.

The significance of the previous discussion is that there exists a maximum absorption coefficient that can be measured using transmission spectroscopy. This could be a drawback to the method if one wanted to measure higher absorption values, say the absorption above the band gap, i.e. for energies greater than the band gap energy. This affected this work because, as the temperature was increased, the absorption increased. So, for some materials, at a high enough temperature, they were completely absorbing, i.e. there was no detectable transmission. This meant that there was a temperature limit

for each sample and also that measurements could not be made over the same range for all samples.

To be more specific, the maximum temperature for the III-V binary semiconductors was about 550 K. The silicon sample was taken up to almost 900 K, as high as the heater could go. The germanium was taken up to 650 K, at which point it became completely absorbing and the transmission was zero for all values of wavelength. This was due to the relatively large thickness of the wafer, around 2 mm. This temperature limit could be increased by decreasing the thickness of the wafer. This is most often accomplished by polishing the wafer until it reaches the desired thickness.

Another limitation was the experimental setup which will be described in more detail in the next section. In particular, the fact that the samples were surrounded by air and not in a vacuum could be a source of error. Oxide layers tend to form more rapidly at higher temperatures, so the surface properties of the materials may have changed appreciably as temperature increased. Using a dewar with a vacuum pump is a possible alternative; the pros and cons of such a setup are discussed in the next section.

II. Experiment

Experimental Procedures: Transmission Measurements

Optical transmission measurements were taken using a Perkin-Elmeir 5000 series FTIR spectrometer. The samples were mounted inside a copper heater block with a one inch round aperture. The block had two “adjective” heater probes powered by a Variac variable transformer. The Variac had a dial to adjust the output current (and consequently the heat). Also attached to the heater block was a K-type thermocouple to monitor the temperature in the heater. The thermocouple was held in place by a small set screw. It was positioned vertically halfway between the two heater probes and approximately 5 cm from the edge of the aperture.

The thermocouple was connected to an “OMEGA 3” temperature sensor which displayed the temperature in degrees C. The transformer was operated manually and the temperature readings were recorded by hand. The temperature response of the transformer-heater block assembly was recorded, stepping up the transformer output in increments of 5%. This was done to determine what dial percentage should be used to obtain the desired sample temperature. The temperature response of the heater is shown in Figure 4.

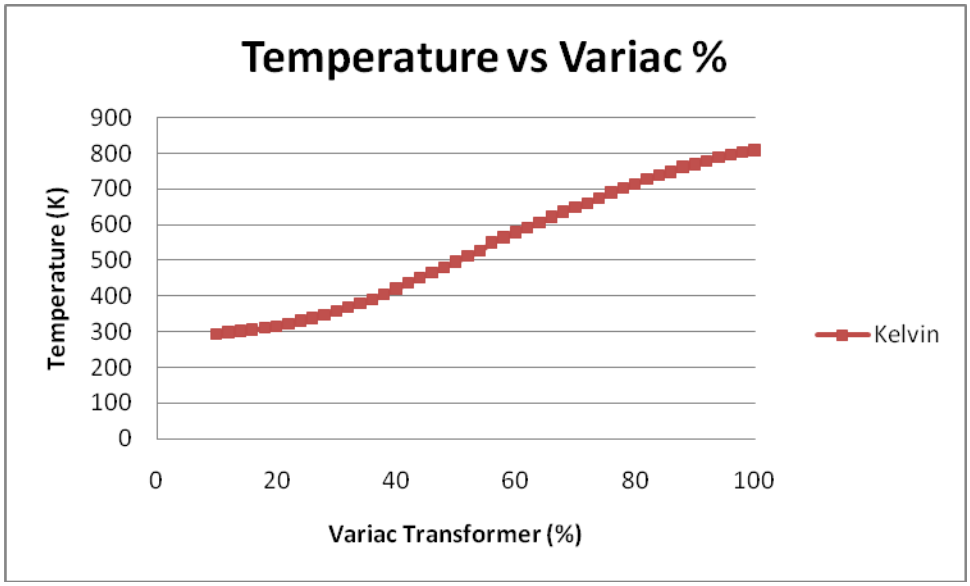

Figure 4. Variable transformer temperature response as a function of dial percentage (or output power)

Shown in Figure 5 is the linear portion of the temperature response. The slope of the curve gives the degrees Kelvin per dial percentage.

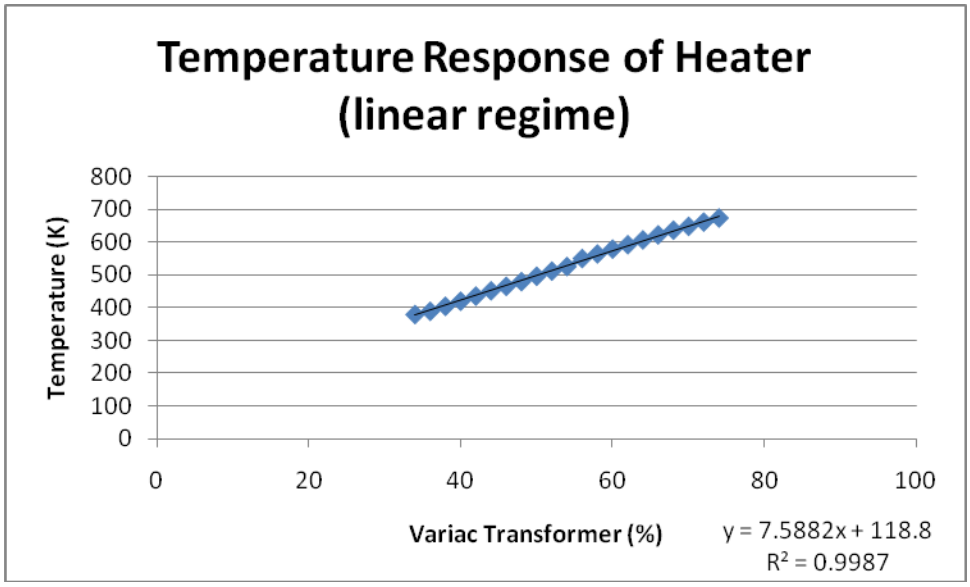

Figure 5. Linear temperature response of the transformer-heater assembly

The value of the slope obtained from the plot is approximately 7.5 K/%. So, to achieve a 50 degree increase, the dial should be increased by 6.67% (50/7.5). Since 6.67 is not a very practical increment, the value used instead was about 5%.

Using this method, the sample temperature could be increased by 50 degrees with a lag time of only about 5 minutes. The heater could have been used with less time between steps, but heating the samples too quickly could have had negative effects. Deformations could form due to the thermal stress, and a change in the structured order within the material would cause a change in the optical properties. So the samples were brought up to temperature relatively quickly, but not so quickly as to be damaging.

With this method, the total time required to take data for a particular sample was approximately one hour. The number of measurements taken from 300 K to 800 K, in steps of 50 degrees, is 10 (800-300=500, 500/50 = 10). At an average time of 5 minutes per measurement, that comes out to about 50 minutes, or roughly an hour. Most often, the last few measurements took longer since the higher temperatures were more difficult to reach. Referring back to Figure 4, this can be seen in the right side of the graph where the curve starts to level off above 700 K.

The samples were heated from room temperature and measurements were taken every 50 degrees, up to the maximum temperature. At each temperature point, a scan was taken using the spectrometer. At first, the maximum temperature was simply chosen to be the highest temperature the heater could go. This seemed like a safe assumption since the melting point of all the semiconductors was far greater than 800 or 900 K. Also, since the

focus of the research was on high temperatures, it would have been ideal to go as high as possible for all samples.

During the first measurement, a GaAs sample was heated to around 800 K. After cooling, significant discoloration was observed. Also, the room temperature spectra taken after heating did not match the data from before. What had not been considered was arsenic dissociation. The change in the appearance of the wafer, and consequently its absorption, was due to the fact that, on the surface, most of the arsenic sites were now vacant and so the material was almost all gallium. This gave rise to a darker, more metallic, or more Gallium-looking surface. It was then found that for GaAs, for instance, the temperature at which arsenic begins to dissociate is about 380 °C or 653 K.

Unfortunately, for all binary semiconductors, even for temperatures far below melting, dissociation can occur. Again this causes a loss of atoms to the surrounding atmosphere, leaving vacancies in the lattice which can change the properties of the material. The surface is the most affected by this and so surface properties like reflectance are very sensitive to these changes. Because of this, maximum temperatures had to be determined for the various materials. Dissociation temperatures for all the III-V semiconductors can be found, but they are all fairly similar to the one stated for GaAs. So, it was decided that the binary compounds (GaAs, GaSb, InAs, and InP) would only be heated to around 550 K to avoid excessive dissociation and subsequent surface damage.

Also, as a safety measure, a fume hood was constructed and used to vent any toxic gas and/or particles away from the sample heater, spectrometer, and the researcher.

The hood was connected to a large pump which contained an air filter. Ideally a dewar could be used to accomplish this purpose. In it, the sample could be contained in a low pressure, low oxygen environment which would discourage any evaporation. Also, since the dewar is self-contained and sealed, it would prevent any gas or particles from immediately escaping into the room air. Unfortunately, since the sample was held in the heater and the heater was connected to the two thermal probes, as well as the thermocouple and translation stage, containing the sample in a dewar would have been very difficult.

III. Results and Analysis

Overview

Temperature dependent transmission data showed significant band gap shifts as well as "dips" for energies below the band gap energy. The absorption data was calculated from the transmission data using the process described in the above sections. The results were compared to previous works for each of the samples. The temperature dependent band gaps were also calculated using the method described earlier. The results agreed well with previous work as to the temperature dependence of the band gap. When plotted, the slopes matched, so the relative change in the band gap with temperature was similar. However all of the temperature dependent band gaps seemed to have an offset that differs from previous works by about 10% on average.

The free carrier absorption was compared with previous work and also compared with theoretical values. In the mid to far infrared range, multi-phonon effects were also observed and their energies were compared with previously observed values as well as theoretical ones.

Calculating the band gap for the materials was not trivial. The method used was found in Schroder[5]. For direct band gap materials, the square of the absorption, α^2 is plotted against energy, hν. The extrapolated intercept on the energy axis (where $\alpha=0$) gives the band gap energy. For indirect band gap materials, the square root of the absorption, $\alpha^{1/2}$, is plotted against energy, hν. Again the extrapolated intercept on the energy axis (where $\alpha=0$) gives the band gap energy.

Alternatively, some sources used the product of the absorption and the energy raised to the respective power to find the band gap. For instance, instead of plotting α^2, one would plot $(\alpha \times h\nu)^2$ and then find the extrapolated intercept at $\alpha=0$. Both of these methods were employed using MatLab and gave similar results. The second method usually gave slightly higher energy values for the band gap.

In evaluating the band gap the difficulty was choosing which points to use for the extrapolation. The "straight" portion of the absorption curve was desirable, but the selection of that portion was nebulous. Eventually what was done was to find the minimum (low energy end) and the maximum (high energy end) of the absorption spectra. The energy at which the absorption was 75% of the maximum (high energy) value was calculated. The energy of the maximum absorption and the energy of 75% value were used to define the line used in the extrapolation.

The plots of absorption and the extrapolation show good agreement between the actual absorption curve and the extrapolated line in the "linear" region. The reliability of the algorithm decreased as the temperature approached the higher temperatures. For these cases, the absorption was so large that the shape of the curve no longer had the linear region near the maximum. This is due to the fact that the absorption was now far exceeding the maximum absorption the spectrometer could measure. So even at the lowest transmission, the part of the curve that was seen was more like the tail and less like a good line. Because of this change in the shape of the absorption curve, the line extrapolated ended up far lower in energy than it should have been.

The curve fitting for the various data points was done using MatLab's curve fitting tool which uses a non-linear least squares algorithm to compute the curve fits. Various functions can be used in this tool including polynomial, exponential, logarithmic, trigonometric, and even custom functions which was useful for evaluating Varshni's equation. To compare different fits, the coefficient of determination, R^2, was recorded from the output of the algorithm. Sometimes, when the shape of the absorption curve changed significantly at the higher temperatures, those data points were left out of the curve fit. Without those points the general band gap vs. temperature plot followed more closely to the expected values at least in their slope and had a better R^2 value (closer to 1).

Results for Silicon (Si 17_3)

Temperature dependent transmission measurements for silicon were taken up to approximately 880 K. The data was taken in two parts, in near infrared region (near infrared) and in the mid-wave infrared region (mid-wave infrared). The near infrared transmission is shown in Figure 6. The absorption edge can be clearly seen shifting to lower energy (to the right) as temperature increases. Additionally, a decrease in the overall transmission was observed for photon energies less than ~0.9 eV. This can also be seen in the transmission in the mid-wave infrared range which is plotted in Figure 7.

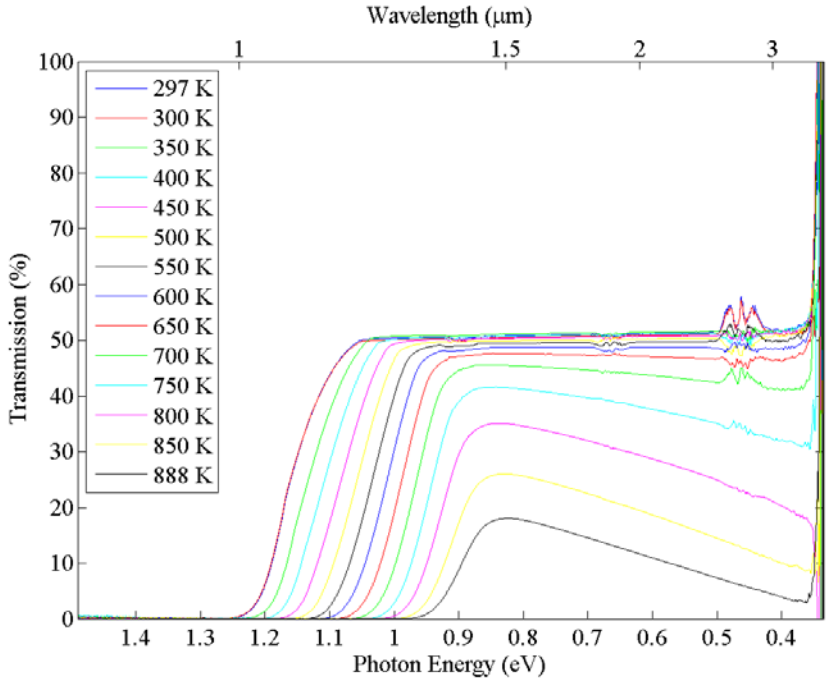

Figure 6. Near infrared transmission versus photon energy for Si at various temperatures

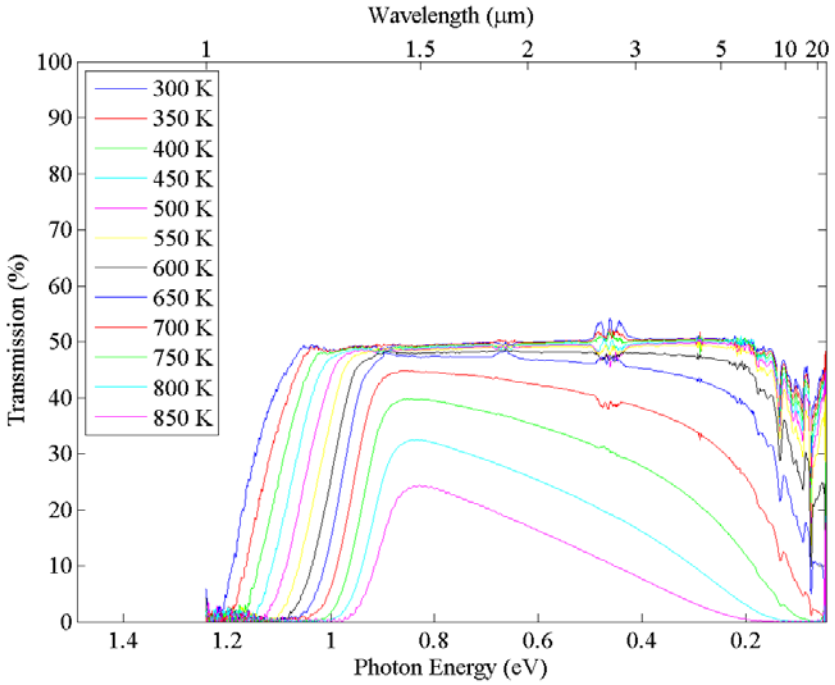

Figure 7. Mid-wave infrared transmission versus photon energy for Si at various temperatures

The absorption in the mid-wave region, wavelength greater than 5 microns, can be explained well by free carrier absorption, phonon absorption, and impurity scattering. The near infrared data provided the best set with which to evaluate the band gap shift. For the mid-wave infrared, the band gap was near the edge of the detector response, and so it was a little noisy. Near the other end of the spectrum around 0.2 eV, however, the mid-wave infrared offered some interesting data, seen on the far right side of the graph. The curve goes from being relatively smooth to having a lot of dips and peaks. These will be associated with phonon peaks in a few pages.

To further analyze the data and compare it to previous work, the absorption coefficient was calculated from the transmission data as described previously. The advantage to looking at the absorption coefficient, α, as opposed to just the transmission is that α is independent of sample thickness. Figure 8 shows a closer view of the band edge and compares the results of this work to previous work by MacFarlane et. al[6]. The graph is plotted as $(\alpha \times h\nu)^{1/2}$ vs. $h\nu$, where $h\nu$ is energy in units of eV.

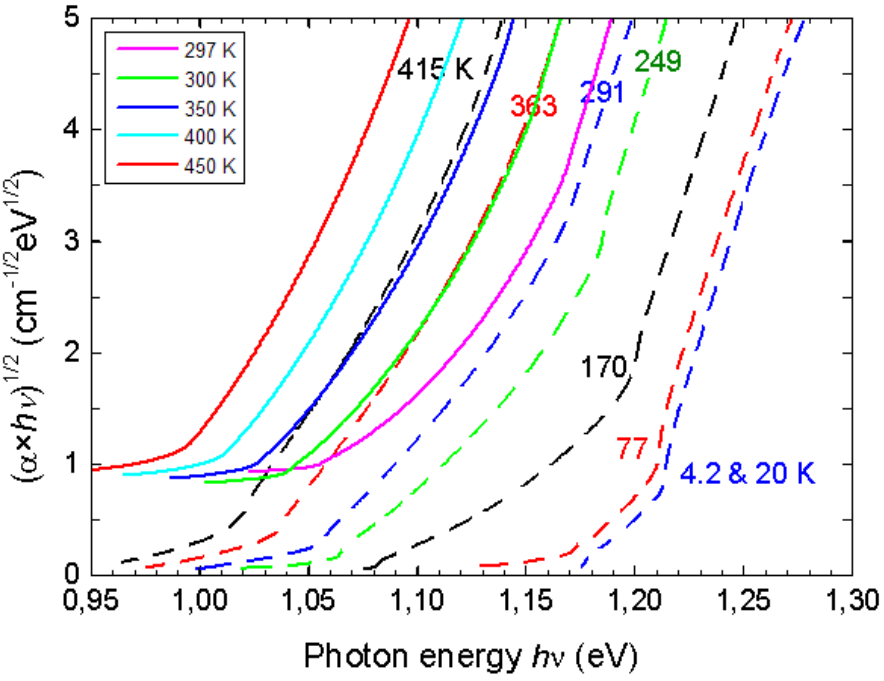

Figure 8. Low level absorption edge of Si versus photon energy at several temperatures comparing previous work (dashed lines) to this work (solid lines)

The dotted lines with the temperatures marked in the plot window are the results of Macfarlane et. al. [6] and were obtained from www.ioffe.ru [7] which is essentially an online version of the book, *Handbook Series on Semiconductor Parameters* (volume 1) [8]. The solid lines and the corresponding legend are the results of this research. The slopes seem to be in good agreement, but there is a shift between the two. The red line labeled 363 (Macfarlane) overlaps the green line (this work) which is 300 K. That seems to imply about a 60 K difference between the two. This could be a result of an error in the temperature measurement of this experiment. This seems unlikely however since the room temperature (297 K) measurements were taken without the heater turned on. Even considering a possible bias in the thermocouple, without the heater on, the sample should have been the same temperature as the surroundings, i.e. room temperature.

The band gap energies were evaluated using the absorption data as described earlier. The results of the extrapolation at temperatures of 300, 600, and 800 K are shown in Figure 9.

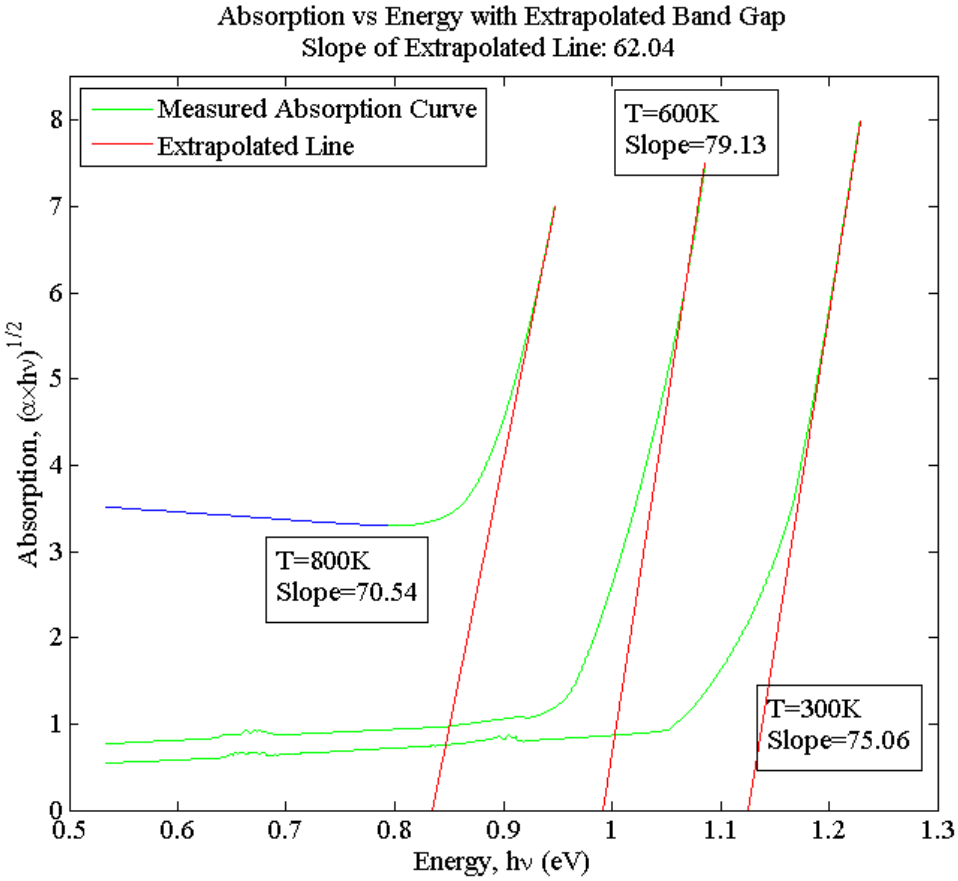

Figure 9. Measured absorption (green) with extrapolated band gap (red) for Si at 300, 600, and 800 K.

At the highest temperature, 800 K, the shape of the absorption curve is significantly different than that at room temperature. The slope is not as steep even where the absorption is a maximum, on the high energy (right-hand) side. The slopes of the extrapolated lines were 75, 79, and 70 for 300, 600, and 800 K, respectively. The changing slope may be due to the fact that the absorption could have increased above the

maximum that could be measured, and it results in more of the band tail being included in the extrapolation. This "pulls" the extrapolated value lower in energy, essentially overestimating the shift in the band gap with temperature.

The results for the band gap shift with temperature for Si are shown in Figure 11 below. As mentioned previously, it is believed that the change in shape of the absorption curve is the reason for the departure from the theory at high temperatures. Varshni's formula is plotted in red, while the measured result is plotted in blue. The last line, in green, is the result of work by Bludau et al [8]. It appears that the data matches the Bludau results better than those of Varshni.

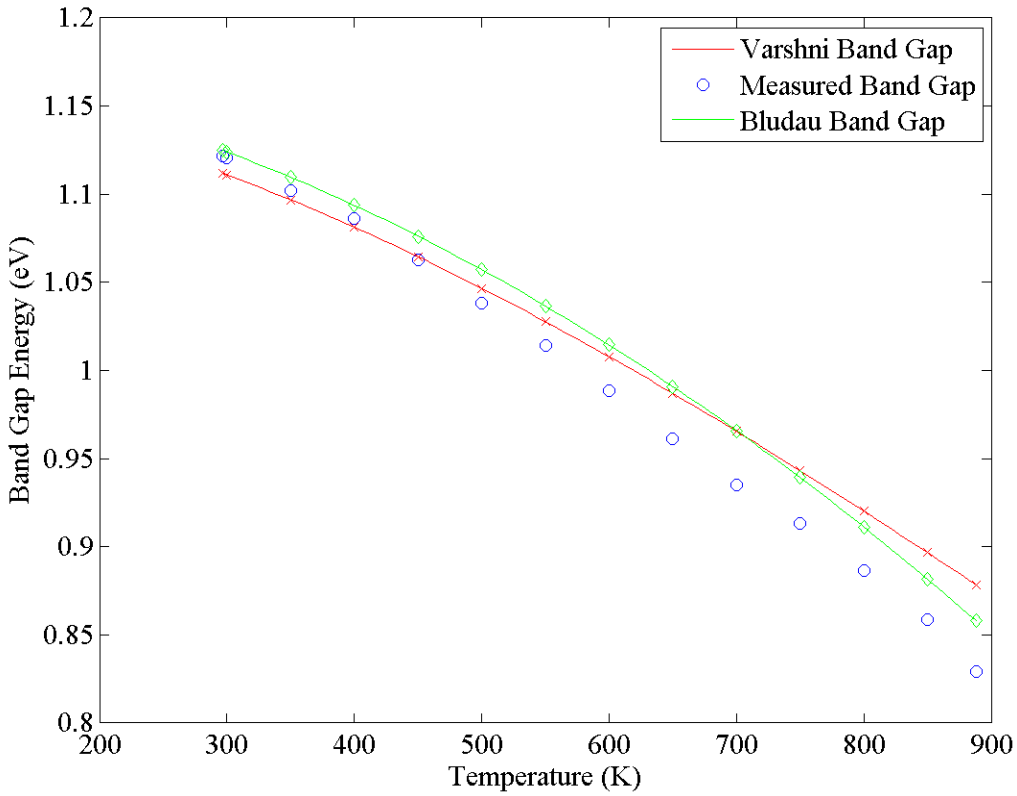

Figure 10. Measured values of the band gap of Si from 300 to 900 K compared to the works of Varshni and Bludau.

Figure 11 shows the absorption at 300 K from 2.5 to 20 microns along with two fits of the data to a polynomial of degree two, i.e. $y = a(x-b)^2 + c$. The results of the fit are listed in Table 1.

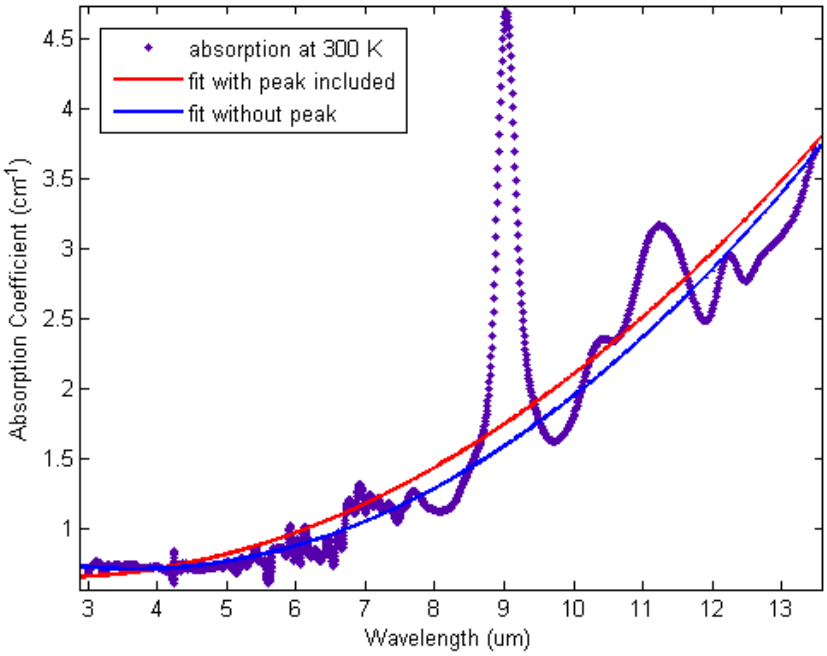

Figure 11. Free carrier absorption versus wavelength for Si from 3 to 13.5 µm at 300 K.

Table 1. Fit parameters for free carrier absorption in Si at 300 K with and without peak due to Oxygen included

	a	b	c	R^2
With Peak	0.02525±0.00181	2.424±0.359	0.6532±0.0335	0.7949
Without Peak	0.03076±0.00069	3.670±0.087	0.7141±0.0068	0.9599

The values in the table (and in all following fit tables) following the '±' sign are based on a 95% confidence interval from the fitting algorithm. The first fit is with all the data points shown, while the second does not include the points in the large peak near 9

microns. This peak is associated with oxygen absorption. As mentioned earlier, the total absorption curve is the superposition of the free carrier absorption and the impurity scattering (and phonon absorption.) For that reason, and in order to get the absorption data to fit to a λ^2 curve, it is helpful to exclude the peaks. The peak was excluded using manually using MatLab by clicking on the plot and choosing a cutoff for the left and right sides.

Since the peak due to oxygen is the only large peak in this wavelength range, it was the only one that was excluded. There are also phonon peaks around 10.4, 11.2, and 12.2 microns, which will be analyzed in following pages. However, since they were not as large as the oxygen peak (and due to the difficulty of manually cutting them out), they were not excluded from the fit. Similar fits were done for all the temperatures measured. The results are plotted on a log-log scale in Figure 12.

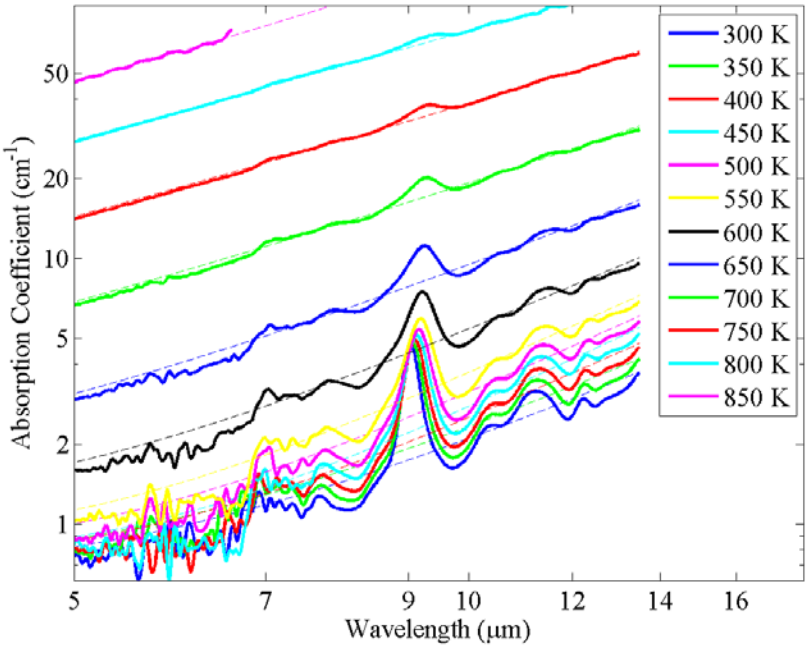

Figure 12. Free carrier absorption for Si from 5 to 13.5 microns from 300 to 850 K.

Results for the lead coefficient (slope of the curve) are listed in Table 2.

Table 2. Fitting parameters for free carrier absorption in Si at several temperatures

Temperature	a (slope)	R^2
300	0.0253±0.0019	0.7948
350	0.0283±0.0019	0.8320
400	0.0375±0.0019	0.8546
450	0.0471±0.002	0.8736
500	0.0482±0.002	0.9013
550	0.0578±0.0021	0.9230
600	0.0693±0.0022	0.9575
650	0.0895±0.0024	0.9831
700	0.1219±0.0025	0.9946
750	0.1785±0.0029	0.9981
800	0.2537±0.0053	0.9987
850	0.8111±0.0193	0.9990

Using the expression given in the theory, the carrier concentration can be extracted from the free carrier absorption. Schroder et al. [9] determined a relation for the absorption in terms of carrier concentration for n-type Si which has the following form:

$$\alpha = 10^{-18} n_0 \lambda^2$$

where n_0 is the carrier concentration and λ is wavelength in μm.

Schroeder's work was done using absorption data taken from 2.5 to 20 microns, so his expression should be valid for wavelengths in that range. Using this expression and the "a" coefficients from Table 2, values for the carrier concentration as a function of temperature can be obtained. Those results are shown in Figure 13.

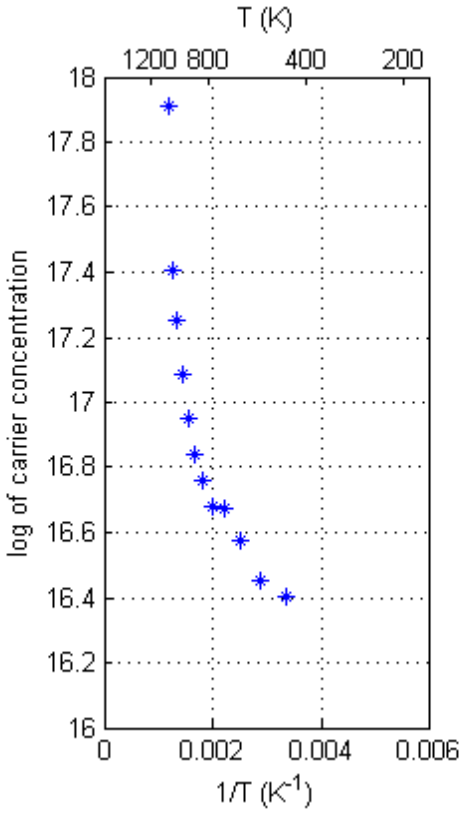

Figure 13. Log of carrier concentration estimated from free carrier absorption versus inverse temperature for Si.

Figure 14 shows the absorption in the mid-wave region and compares it to the result of Collins and Fan [10]. A good amount of overlap can be seen between the two spectra. All of the peaks observed in the previous data can be seen in the data from this work. These peaks correspond to the various phonon frequencies which are listed in Table 3.

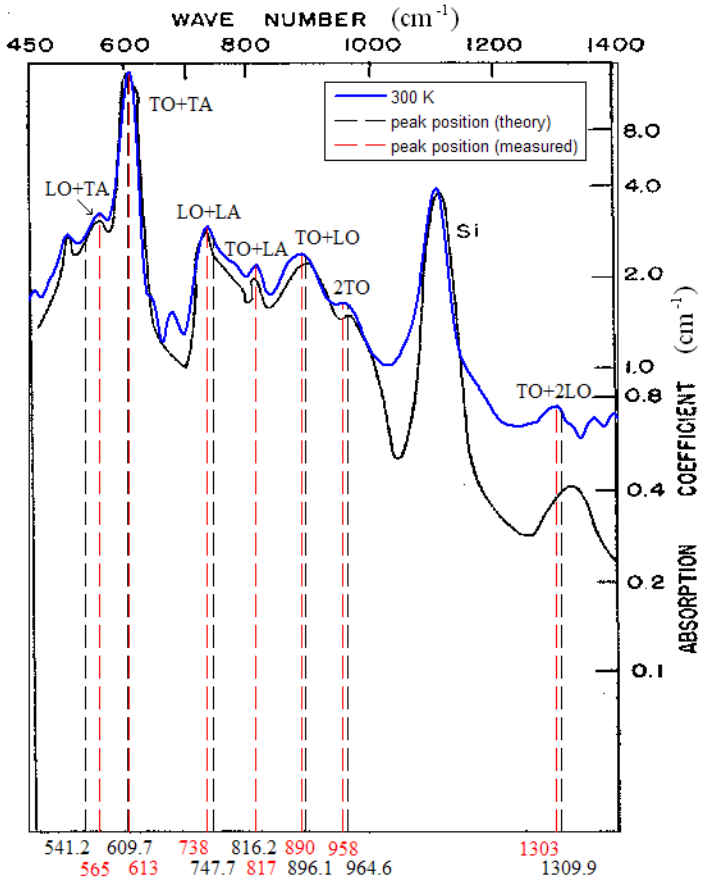

Figure 14. Multiphonon absorption in Si from Collins and Fan[10] (black solid line) and this work (blue solid line) with theoretical (black dashed lines) and measured (red dashed lines) phonon peak positions

Table 3. Theoretical and measured single and multiple phonon frequencies for Si

Phonon Name		TA	LA	TO	LO	LO+ TA	TO+ TA	LO+ LA	TO+ LA	TO+ LO	2TO	TO+ 2LO
frequency (cm^{-1})	calculated	127.4	333.9	482.3	413.8	541.2	609.7	747.7	816.2	896.1	964.6	1309.9
	observed	N/A	N/A	N/A	N/A	565	613	738	817	890	958	1302.5

Here TA is the transverse acoustical phonon, LA is the longitudinal acoustical phonon, TO is the transverse optical phonon, and LO is the longitudinal optical phonon.

The two plots agree well with the exception of the right side of the graph, i.e. for wavenumbers between 1000 and 1400. In this region, the absorption in the sample from this work is greater than that of Collins and Fan [10]. A possible explanation for this is that there may be a greater concentration of impurities in the silicon sample from this work compared to the sample used by Collins and Fan[10]. Greater impurity concentrations would mean more free carriers at room temperature which would cause more absorption. Collins and Fan [10] also measured absorption at 5, 77, 300, and 412 K. Their results are compared with data from this work in Figure 15.

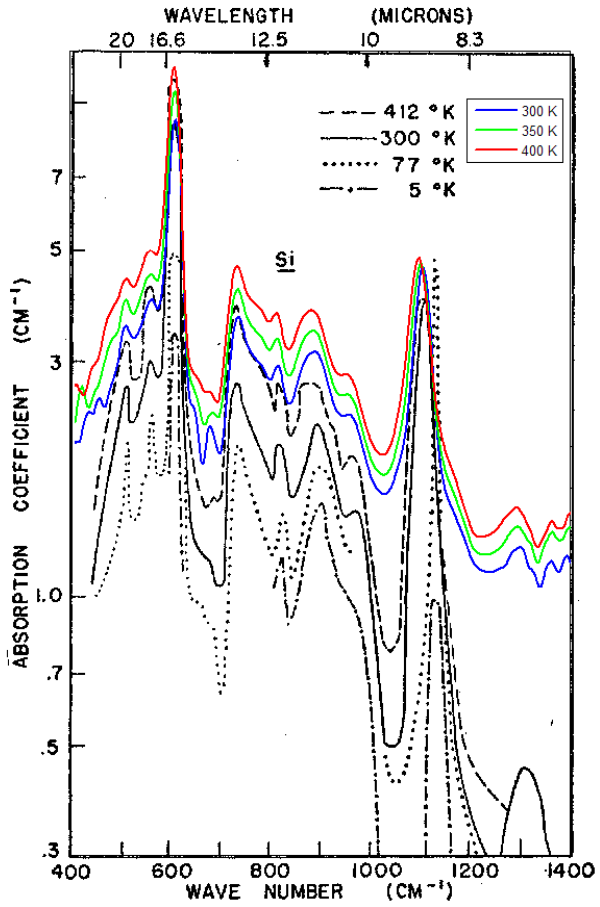

Figure 15. Multiphonon absorption in Si at several temperatures with previous work [10] (black) and present work (colored)

The peak seen around 1100 cm^{-1} is due to impurity scattering, more specifically oxygen. The samples used by Collins and Fan [10] were grown in a vacuum, which would have greatly decreased the concentration of oxygen atoms available during growth and therefore resulted in a purer sample. The smaller concentration of oxygen defects in the vacuum grown samples results in a smaller peak at 1100 cm^{-1}, whereas the sample used in this research had substantially more absorption at that frequency. The oxygen peak also does not change as much with temperature as do the phonon peaks. This is due to the fact that the phonon peaks are affected by lattice expansion whereas the oxygen atoms are not.

Results for Germanium (Ge Window)

Temperature dependent transmission measurements for germanium were taken up to approximately 650 K. The data was taken in two parts, in near infrared region (near infrared) and in the mid-wave infrared region (mid-wave infrared). The near infrared transmission is shown in Figure 16. As expected, the absorption edge can be clearly seen shifting to lower energy (to the right) as temperature increases. Additionally, a decrease in the overall transmission was observed for photon energies less than ~0.55 eV. This can also be seen in the transmission in the mid-wave infrared range which is plotted in Figure 17.

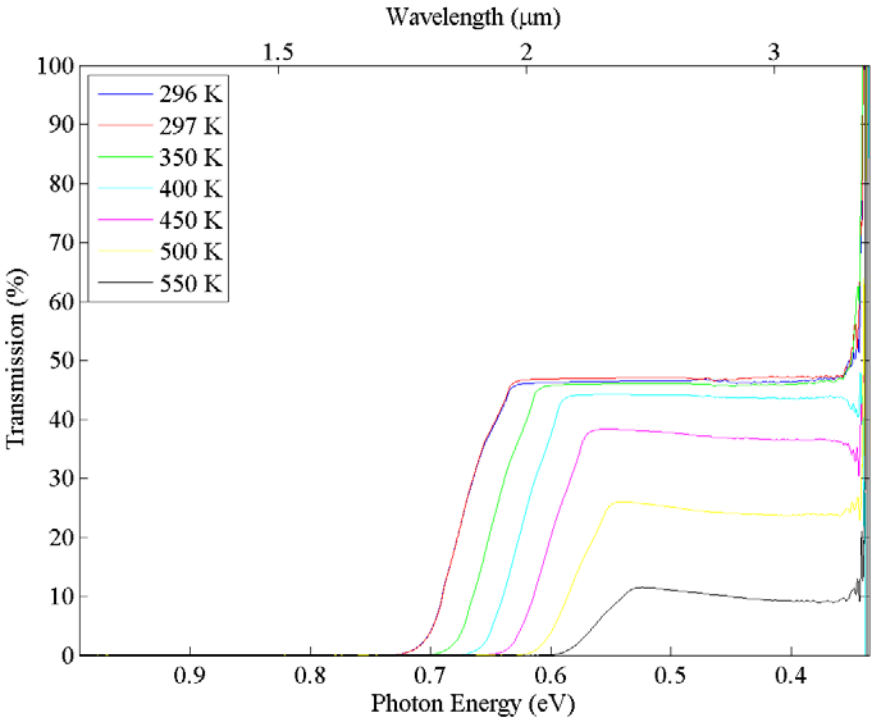

Figure 16. Near infrared transmission versus photon energy for Ge at several temperatures

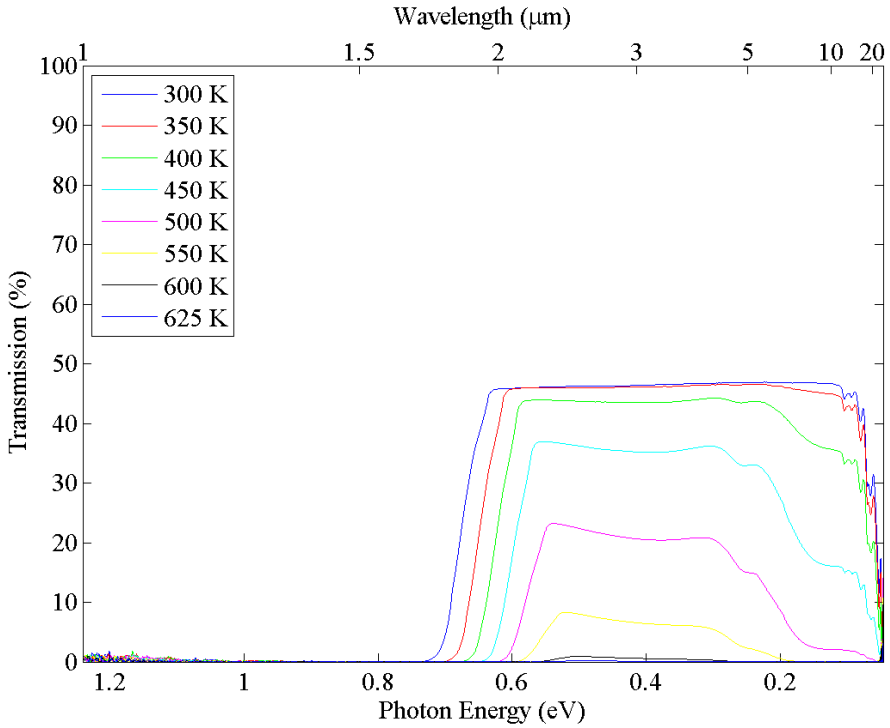

Figure 17. Mid-wave infrared transmission versus photon energy for Ge at several temperatures

The band gap shift can be seen in both the near infrared and mid-wave infrared data and could have been calculated using either set. However, the near infrared was used and gave good results. The results of the band gap calculation for 300, 400, and 550 K are shown in Figure 18.

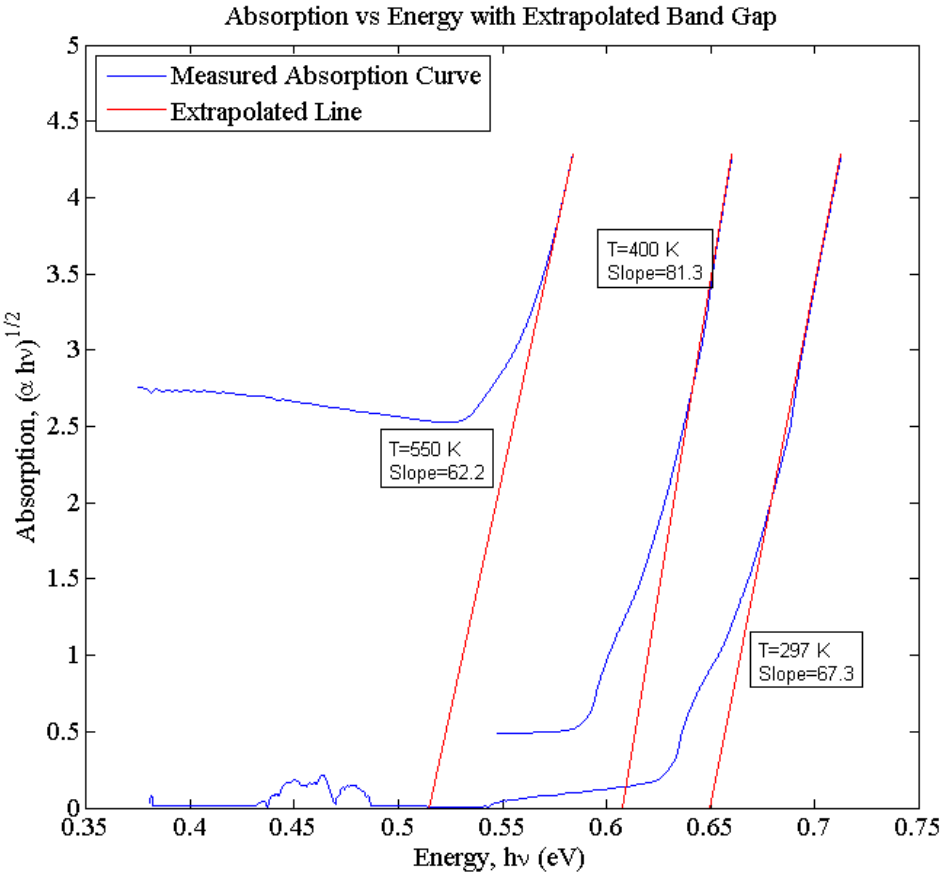

Figure 18. Absorption (blue) with extrapolated band gap (red) for Ge at 297, 400 and 550 K

The band gap could not be calculated for temperatures greater than ~550 K since the shape of the transmission curve changed drastically and did not show a well defined edge. As in the case of Si, the possible error in the extrapolation for the band gap increases with temperature due to the increased contribution of the indirect band gap phonon "tail".

At 297 K, the extrapolated line fits the measured curve very well (for energies greater than 7eV and neglecting a slight bend in the curve around 6.75 eV.) The slope of the extrapolated line has been included to show that shape of the absorption curve near the maximum of the absorption, on the high energy (right-hand) side, can greatly affect the calculated band gap. The measured temperature dependence of the band gap is plotted in Figure 19 and compared to the results of Varshni.

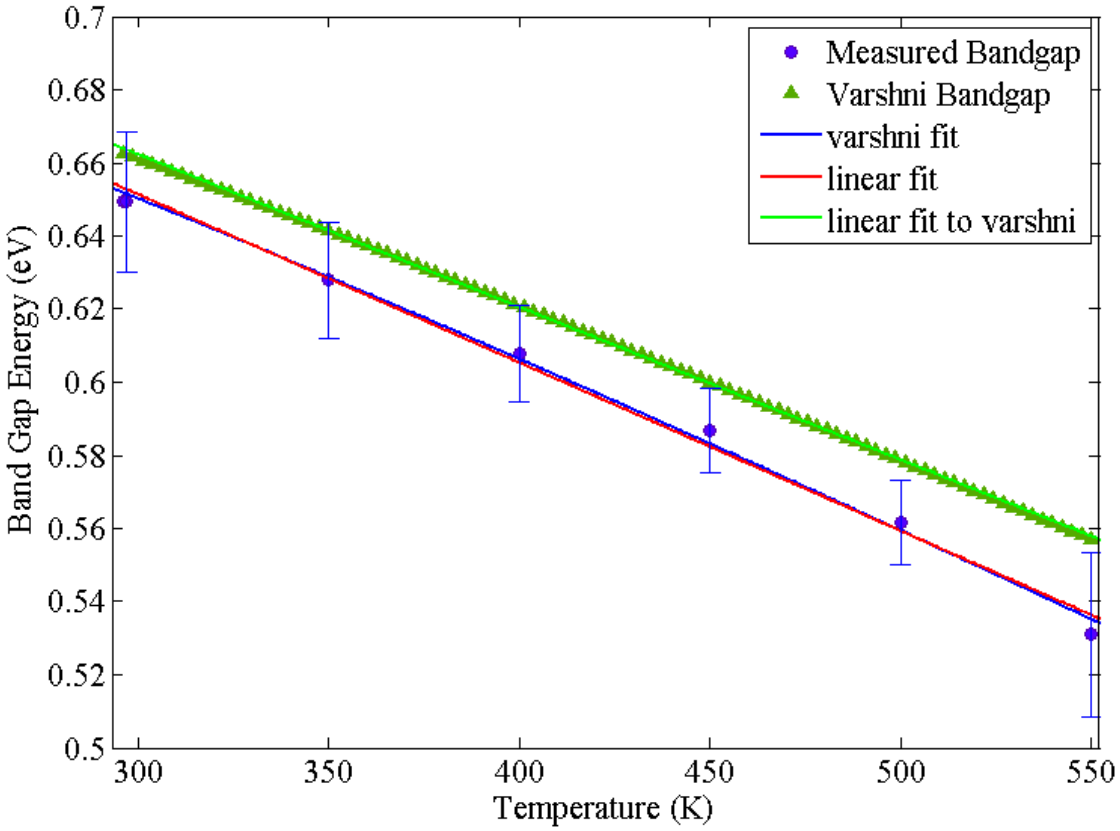

Figure 19. Band gap shift versus temperature for Ge from 300 to 550 K.

The difference between the slopes of the 400 and 550 K line is ~19. With a height in "absorption" $((\alpha \times h\nu)^{1/2})$ of about 4 that equates to a lateral displacement difference of about 0.015 eV. Standard deviations were calculated for the slopes of the interpolated

lines, based on the average slope. To determine an uncertainty in the band gap energy, the maximum of the absorption curve was divided by the maximum and minimum slopes (calculated slope ± std. dev.). Those uncertainties are included in the form of error bars in Figure 19 which shows the band gap shift versus temperature. The fitting parameters from the data in Figure 19 are listed in Table 4.

Table 4. Fitting parameters for the temperature dependence of the band gap in Germanium

Linear Parameters	b (eV)	a (eV/K)	————	R^2
Linear fit to Measured	0.806±0.054	-5.049±1.26e-4	————	0.9689
Linear Fit without 550 K	0.778±0.015	-4.283±0.36e-4	————	0.9979
Linear fit to Varshni	0.787±0.004	-4.170±0.10e-4	————	0.9997
Varshni Parameters	$E_g(0)$ (eV)	α (eV/K)	β (K)	R^2
Varshni fit to Measured	0.711±0.040	-7.897±13e-4	826.2±2527.2	0.9995
Varshni fit to Measured with β fixed	0.733±0.008	-4.986±0.30e-4	235 (value set)	0.9989
Actual Varshni	0.742	-4.8e-4	235	N/A

While the band gap shift is not entirely consistent with the results of Varshni, it seems to follow the same trend. The slopes are very similar for the two sets of data, especially if the data point at 550 K is excluded. Still, the room temperature (300 K) band gap for both sets of data should be very close, but instead they differ by about 11 meV. This is the same order of magnitude as the variation in the slope of the extrapolated band gap lines (~15 eV). However, that is most likely not the source of the error, since all the extrapolations would have to deviate in the same manner, increasing in energy. Also, this

sort of offset seems to be present in the other samples as well, suggesting a systematic error rather than a simple statistical one.

To look more closely at the absorption edge, results for germanium measured by Macfarlane et. al. [11] at temperatures of 20, 77, 195, 249, and 291K are plotted in Figure 20 and compared with the data from this work at 300, 350, and 400 K.

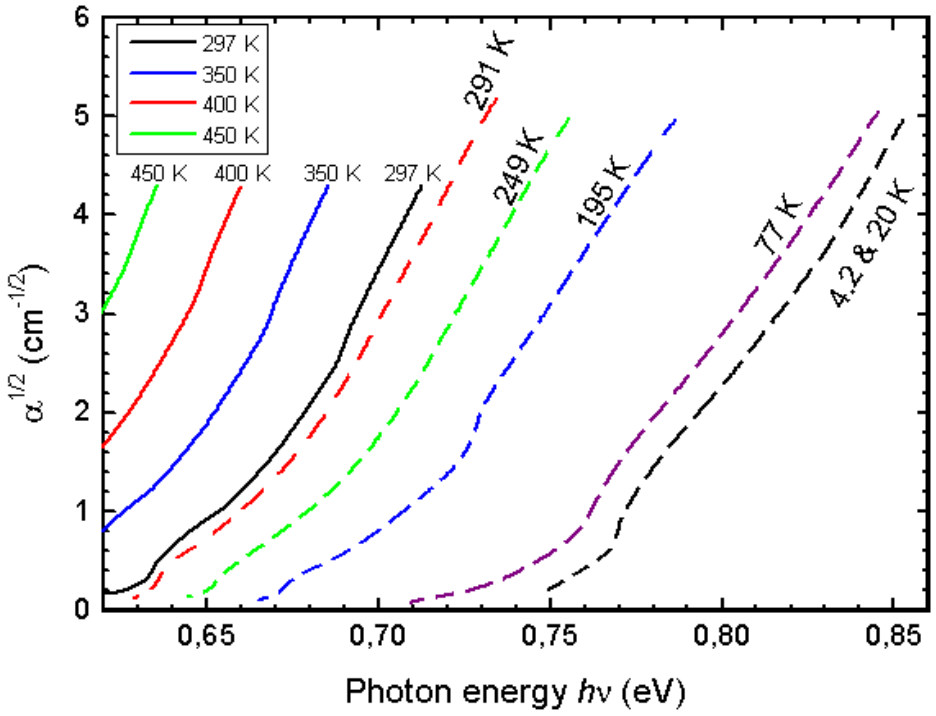

Figure 20. Low level absorption edge in Ge at several temperatures

The results of Macfarlane et. al.[11] are shown as dashed lines and the results of this work are shown as solid lines with the corresponding temperatures in the legend in the top left corner. This comparison seems to indicate a fairly good correlation between previous work and this work, indicating that the measured data may be reliable. The source of error then, is most likely the calculation of the band gap from the measured data.

Multiphonon absorption in Ge was measured by Collins and Fan[10] and is shown along with the results of this work for 300 K in Figure 21. Both of the axes are in units of cm^{-1}. The results of this work are plotted as a solid blue line while the previous work is plotted as a solid black line.

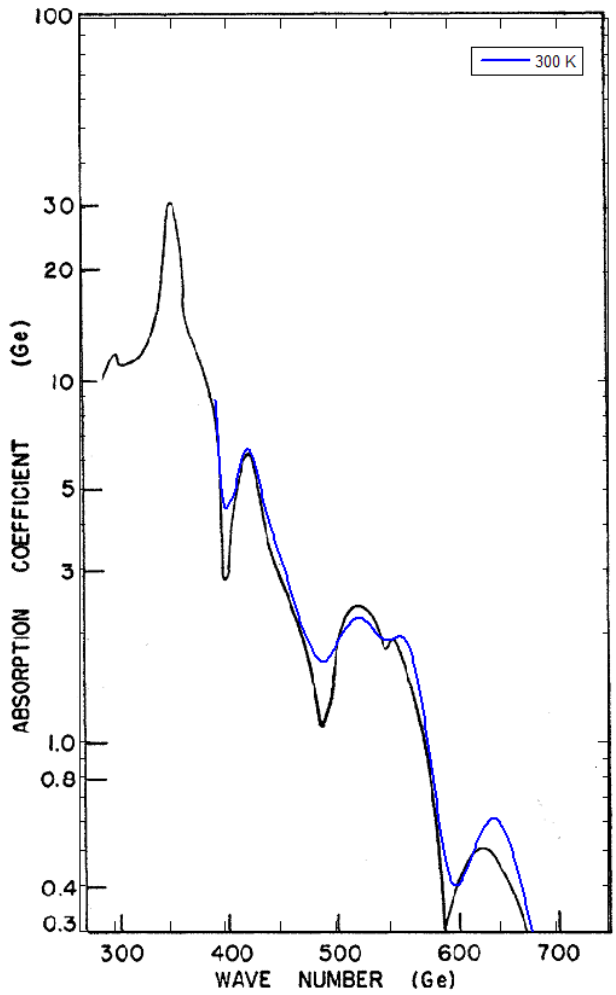

Figure 21. Low frequency multi-phonon absorption in Ge at 300 K

The two can be seen to agree very well both in phonon peak position and height with the possible exception of the peak at 620 cm^{-1}. This adds credibility to the data taken and leads one to think that the spectrometer used is indeed reliable and was giving accurate frequency data.

Collins and Fan[10] also took temperature dependent measurements at 5, 77, 300, and 362 K. The results from this work at 300, 350, and 400 K are plotted with those in Figure 22.

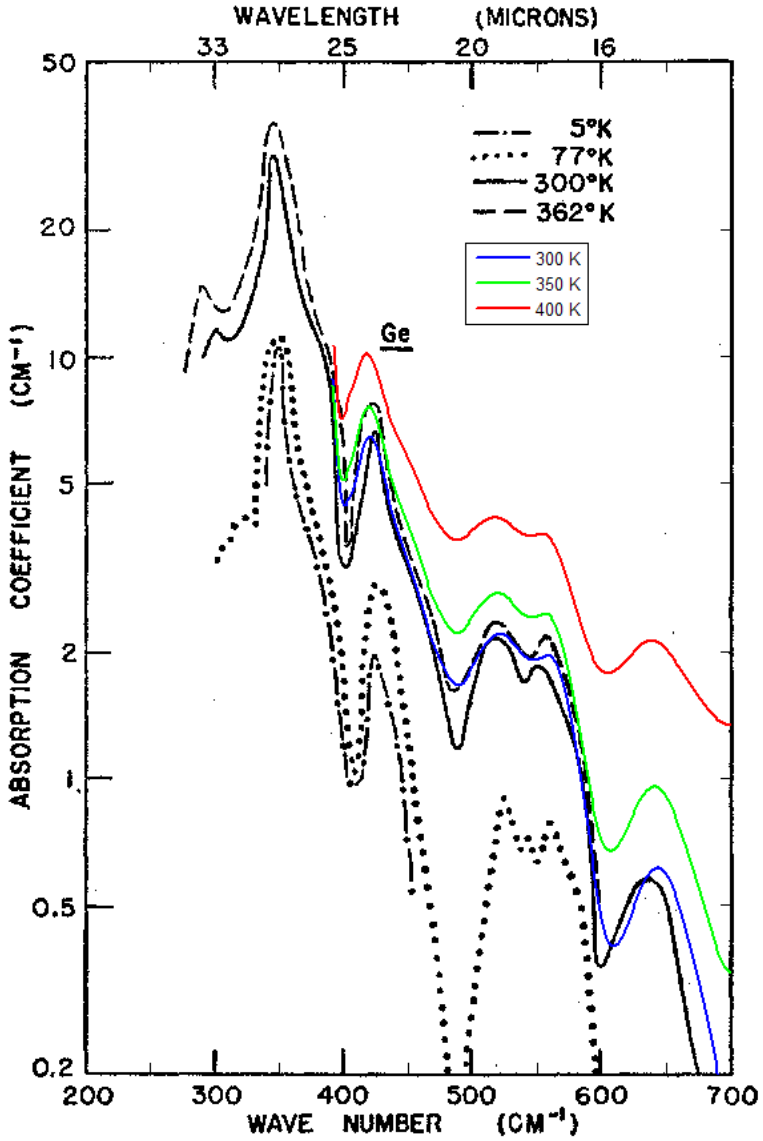

Figure 22. Low frequency multi-phonon absorption in Ge at several temperatures

Results for Undoped Gallium Arsenide (GaAs 82)

Temperature dependent transmission measurements for the first GaAs sample were taken up to approximately 850 K. The near infrared transmission is shown in Figure 23.

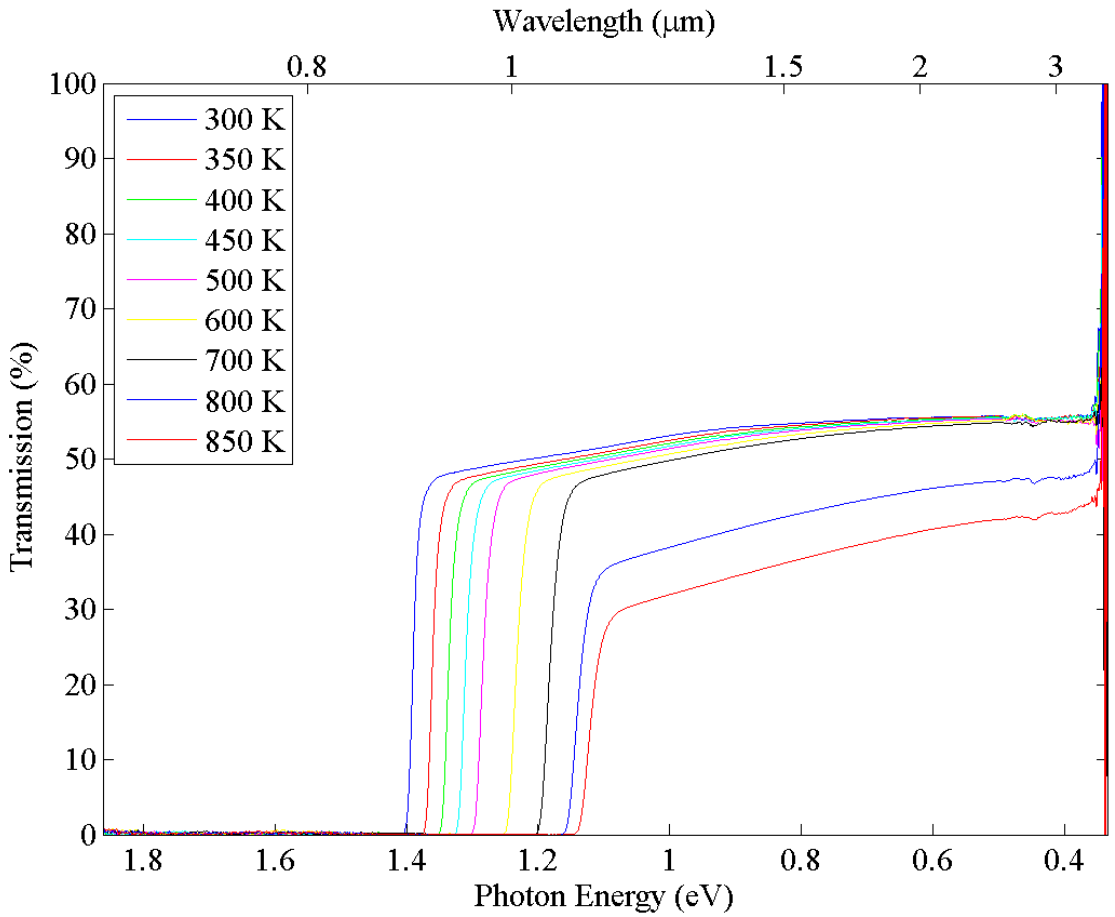

Figure 23. Near infrared transmission versus photon energy for GaAs at several temperatures

Again, the absorption edge can be clearly seen shifting to lower energy (to the right) as temperature increases. Also, a decrease in the overall transmission was observed for photon energies less than ~1.1 eV starting at about 800 K. However, this absorption does not appear to be due to free carriers, as was the case with Si and Ge, because the

transmission is gradually increasing with wavelength (to the right in the figure). So the absorption would be decreasing with increasing wavelength which does not fit the free carrier absorption theory. As mentioned previously, as the temperature of the GaAs sample rose above ~350 K, significant arsenic dissociation occurred. Because of this the surface of the GaAs would have been composed of more gallium than arsenic, and therefore would have more gallium-like properties. Since the reflectivity of gallium is higher than that of GaAs, the drop in transmission could be explained by a reflective loss instead of a loss due to real absorption.

The band gap of GaAs was calculated as a function of temperature using the method described earlier. The absorption and extrapolation curves are shown for 300, 500, and 700 K in Figure 24.

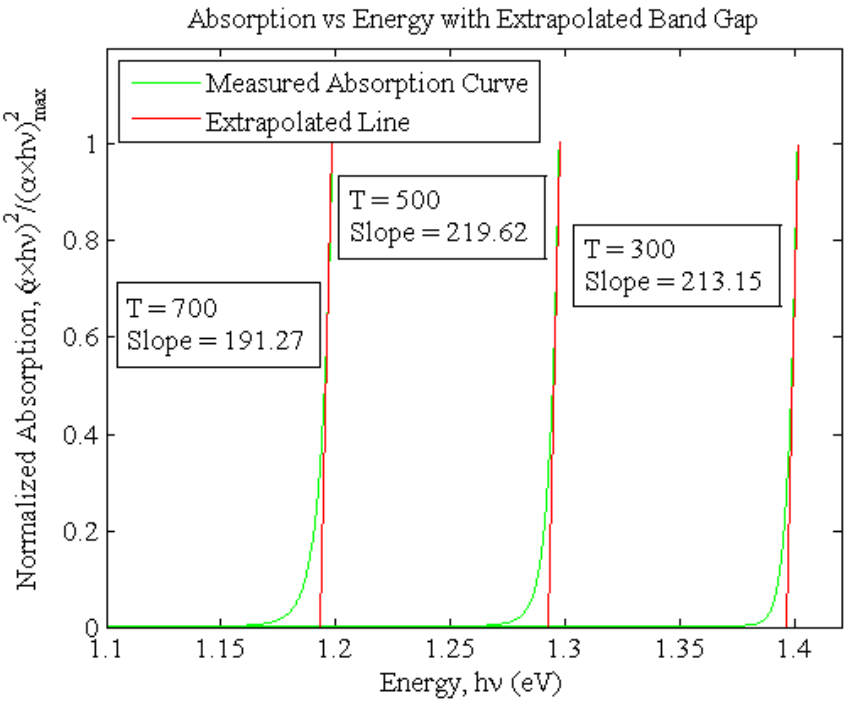

Figure 24. Absorption spectra (green) with extrapolated band gap (red) for GaAs at 300, 500 and 700 K.

For this plot, the curves were normalized by dividing by the maximum value of the absorption at 300 K. All three curves were divided by this same maximum so that their magnitudes relative to each other would not change. All of the slopes are fairly similar, but do increase slightly with temperature. As previously mentioned, the measurements at very high temperatures may not have been reliable due to the arsenic dissociation. For that reason, the data points at 800 and 850 K were left out of the band gap analysis.

The band gap vs. temperature data was analyzed using both a linear fit and a Varshni curve. Those results along with the expected Varshni points are plotted in Figure 25.

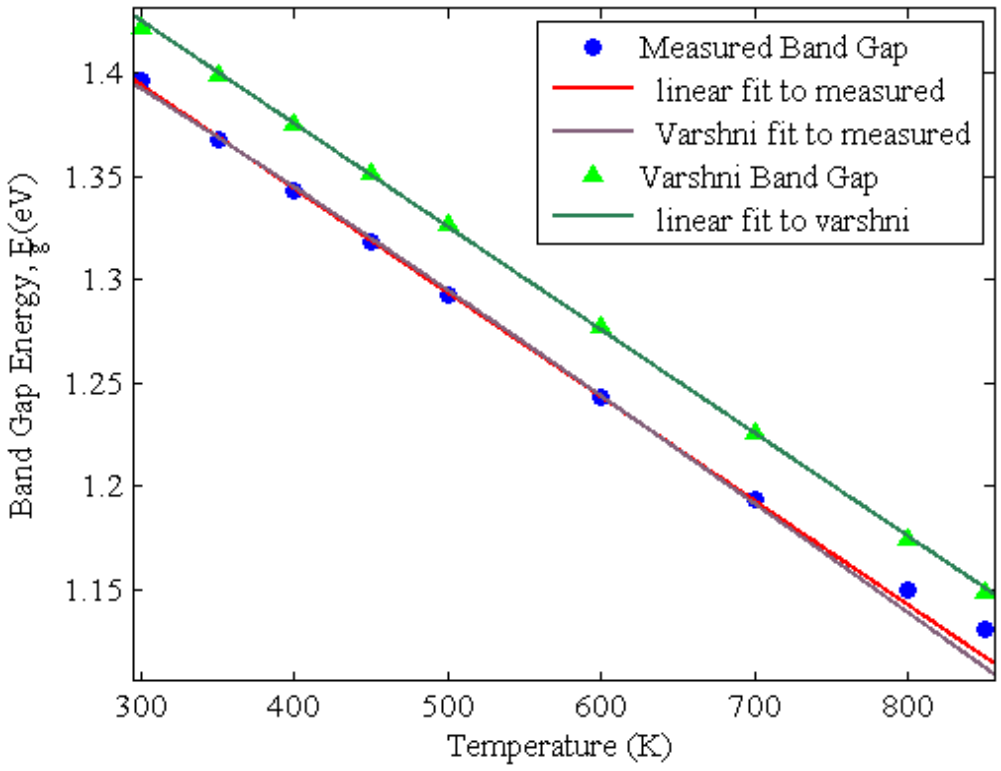

Figure 25. Band gap shift versus temperature for GaAs from 300 to 850 K

The data for the fit parameters is listed in Table 5. Again, all of the measured band gap values are less than the expected ones. On average the difference between the two is 0.03 eV. The linear fits to both the measured band gap and the Varshni band gap are very similar. The slopes only differ by ~1e-6 and the offsets are different again by about 0.03 eV.

Table 5. Fitting parameters for the temperature dependence of the band gap in GaAs

Linear Parameters	b (eV)	a (eV/K)	————	R^2
Linear fit to Measured	1.545±0.004	-5.042±0.09E-4	————	0.9997
Linear fit to Varshni	1.575±0.004	-5.000±0.07E-4	————	0.9997
Varshni Parameters	$E_g(0)$ (eV)	α (eV/K)	β (K)	R^2
Varshni fit to Measured with β fixed	1.4911±0.007	-5.536±0.20E-4	204 (value set)	0.9990
Actual Varshni	1.519	-5.405E-4	204	N/A

Results for Doped Gallium Arsenide (GaAs WV13120-Si_2)

Temperature dependent transmission measurements for an n-type GaAs sample doped with silicon were taken up to approximately 550 K. The mid-wave infrared transmission is shown in Figure 26. Free carrier absorption can be seen for wavelengths in the mid-infrared starting at about 5 microns, while some multiphonon effects are visible further out, from about 19 microns on.

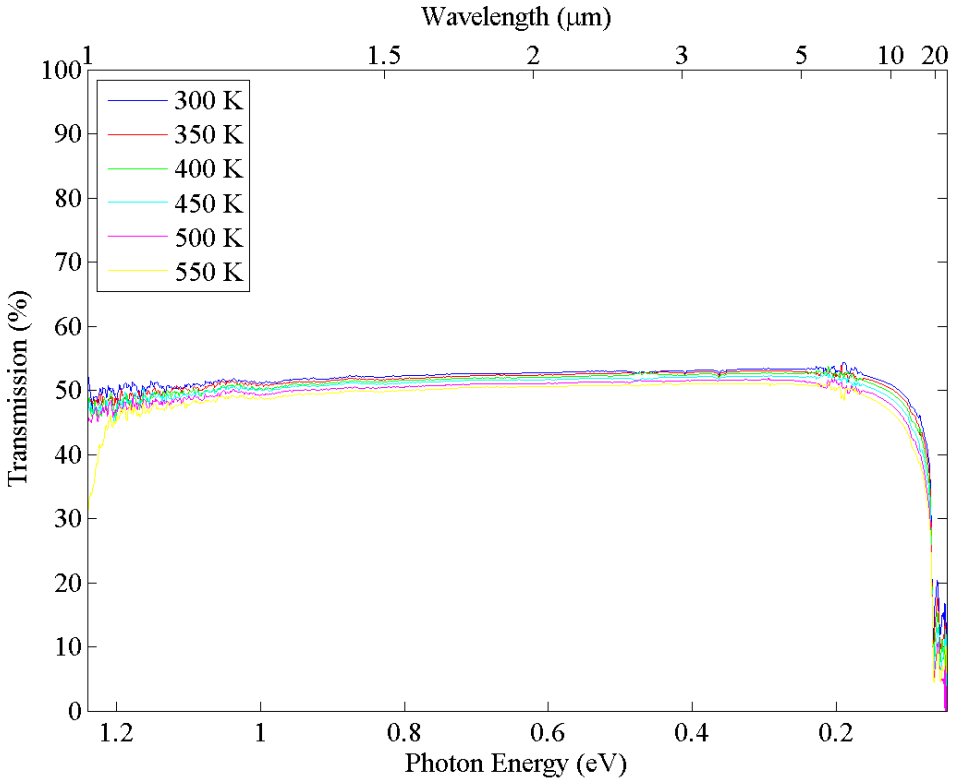

Figure 26. Mid-wave infrared transmission versus photon energy for GaAs at several temperatures

As with silicon, the absorption curves were fit to a general polynomial of degree two in order to verify the predicted λ^2 dependence. Those results are plotted in Figure 27 and the fit parameters are listed in Table 6.

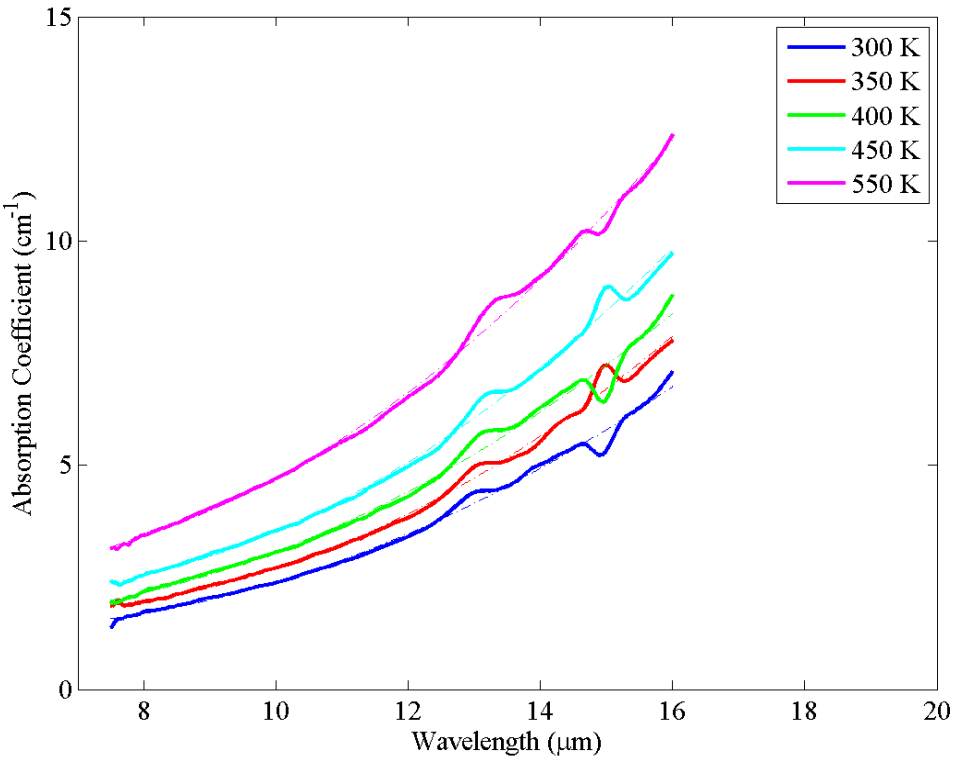

Figure 27. Free carrier absorption in GaAs at 7.5 to 16 μm from 300 to 550 K

Table 6. Free carrier absorption fit parameters for GaAs from 300 to 550 K

Temperature (K)	a (slope)	R^2
300	0.0469± 0.0013	0.995661
350	0.0631± 0.0013	0.996599
400	0.0533±0.0019	0.993773
450	0.0702±0.0015	0.997153
500	0	0
550	0.0759±0.0017	0.997647

Multiphonon absorption is believed to be present in the data at around 13 and 15 microns (seen in Figure 27 as slight bumps and/or dips) and at and beyond 19 microns (seen in Figure 26 as large dip in transmission on the low energy end (right hand side)).

Unfortunately, since this was near the edge of the detector's spectral range, the data is not entirely reliable. Even in the plots shown in Figure 27, for some temperatures there are peaks around 15 microns, but for other temperatures those are valleys. The noise in the data and the inconsistency are worse for wavelengths greater than 19 microns and so the phonon peaks could not be accurately identified.

Results for Gallium Antimonide (GaSb 03055_2)

Temperature dependent transmission measurements for an undoped (not intentionally doped) GaSb sample were taken up to 650 K. The mid-wave infrared transmission is shown in Figure 28. The sample was completely absorbing by about 700 K.

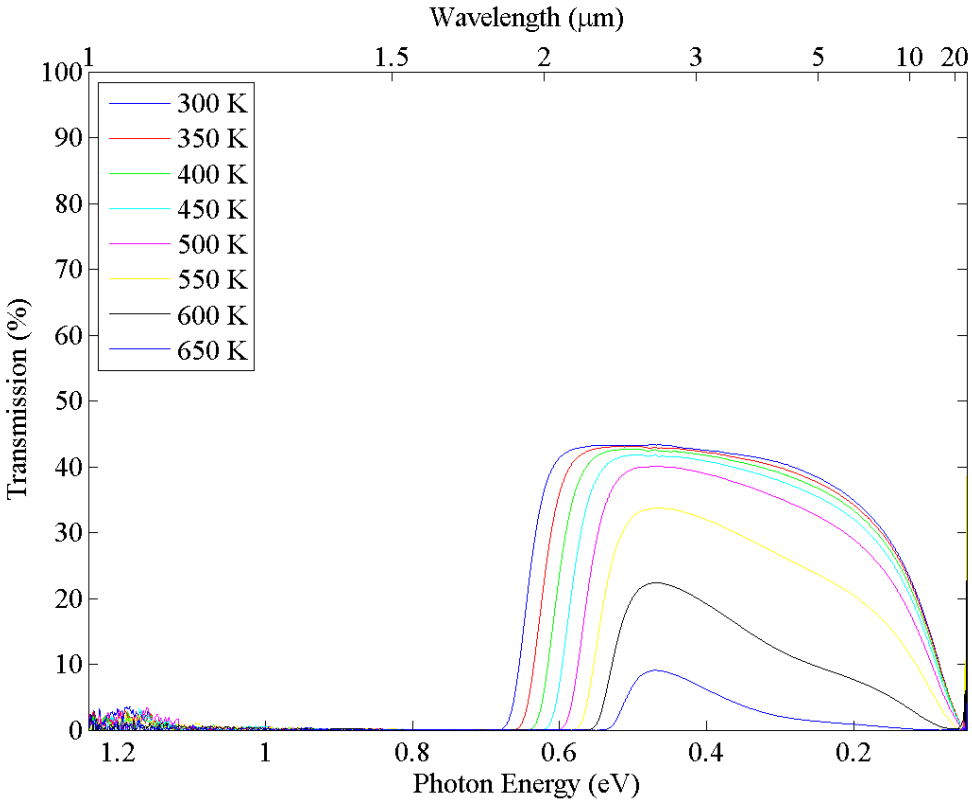

Figure 28. Mid-wave infrared transmission spectra versus photon energy for GaSb at several temperatures

The band gap shift is easily seen in the spectra, though from the shape of the different temperature curves, it appears the 600 and 650 K curves may not give a good value for the band gap. The slope of the extrapolated band gap did have a fairly large variation with temperature. On average, the slopes differed from the mean by about 15%. The extrapolated lines and measured curves for three temperatures are shown in Figure 29 along with their normalized slopes.

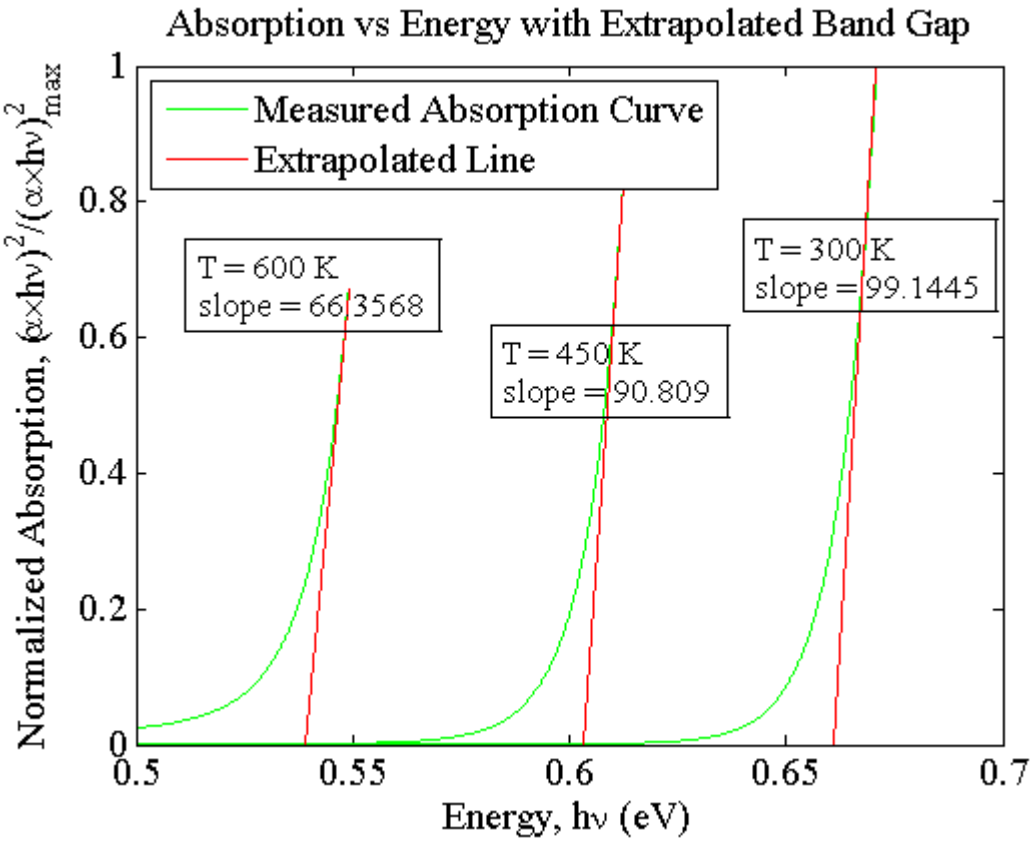

Figure 29. Absorption spectra (green) with extrapolated band gap (red) for GaSb at 300, 450 and 600 K.

The temperature dependence of the band gap is compared to the results of Wu and Chen [12] who used Varshni's equation and determined parameters based on a fit to their data. Wu and Chen [12] only took measurements up to 300 K. There is a considerable

difference between their data and the results of this work. The band gap is plotted versus temperature in Figure 30 along with the results of Wu and Chen [12]. As with many of the other samples, the observed energies are less than the expected values, but the slopes agreed. In this case the slopes differed by about 1e-4 and the offset was about 0.07 eV.

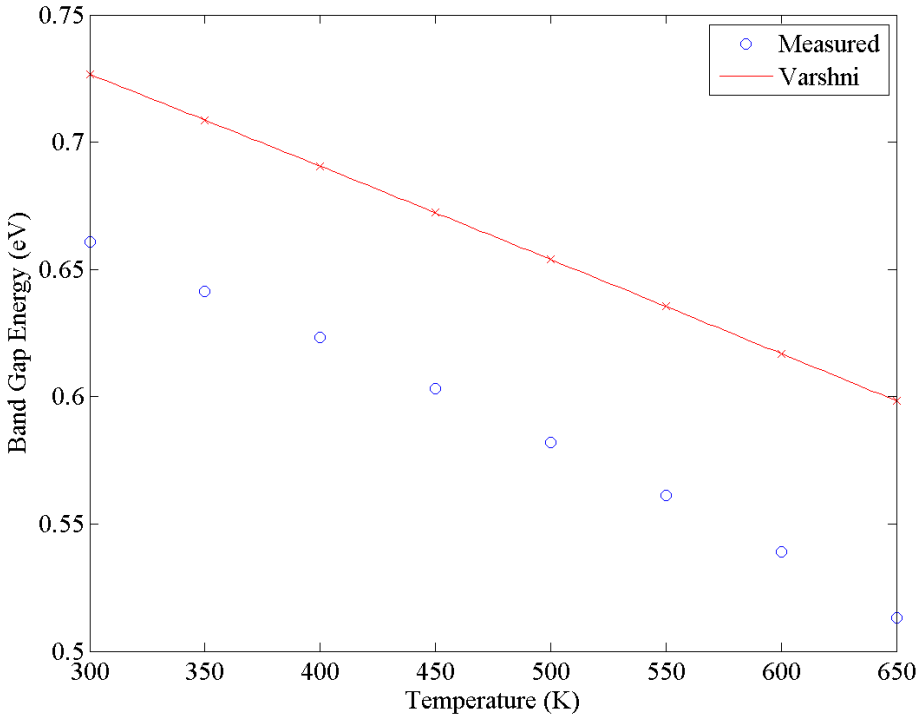

Figure 30. Band gap energy verses temperature for GaSb from 300 to 650 K

The curvature seen at wavelengths greater than about 5 microns is due to free carrier absorption while the dip from about 2.5 to 5 microns is most likely due to impurity scattering. The possible types of impurities and the temperature dependence of their contributions were not investigated. The free carrier absorption was evaluated from 7 to 20 microns. Again the observed absorption curves were analyzed using a least squares method with a general polynomial of degree two. The results are plotted in Figure 31 and the fit parameters are listed in Table 7.

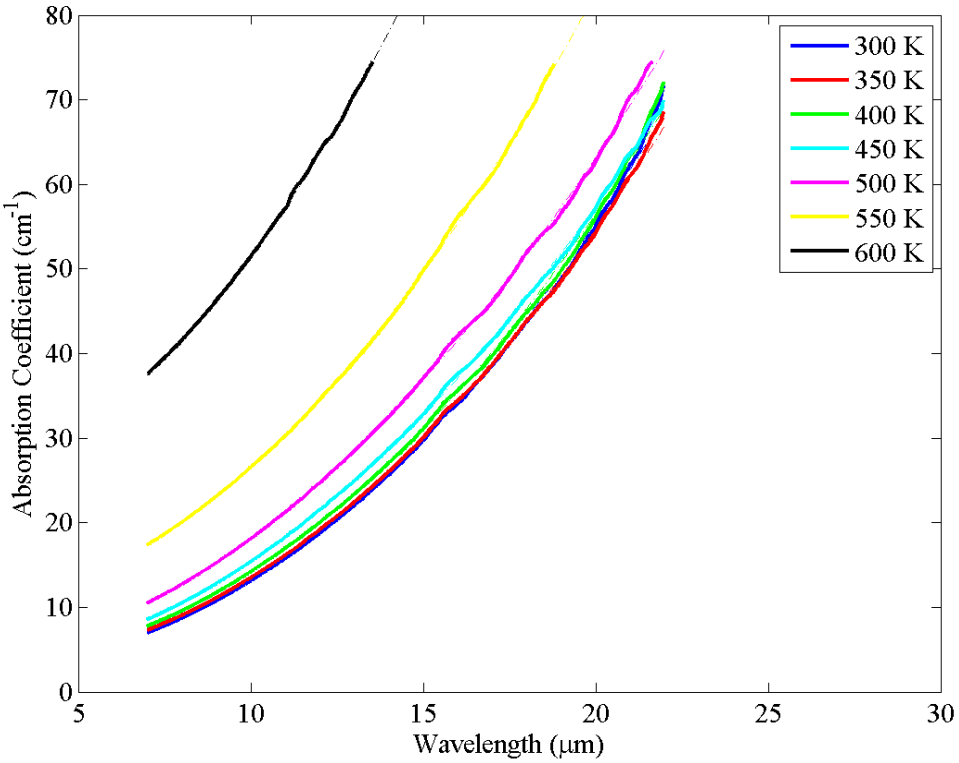

Figure 31. Free carrier absorption in GaSb for 7 to 20 microns from 300 to 600 K

Table 7. Free carrier absorption fit parameters for GaSb from 300 to 600 K

Temperature (K)	a (slope)	R^2
300	0.1810±0.0014	0.9994
350	0.1629±0.0008	0.9998
400	0.1702±0.0015	0.9994
450	0.1469±0.0007	0.9999
500	0.1516±0.0010	0.9998
550	0.2003±0.0010	0.9999
600	0.2813±0.0032	0.9998

Results for Doped Indium Phosphide (InP R41182-S_3)

Temperature dependent transmission measurements for an intentionally doped indium phosphide sample doped with sulfur were taken up to 500 K. The near infrared transmission is shown in Figure 32.

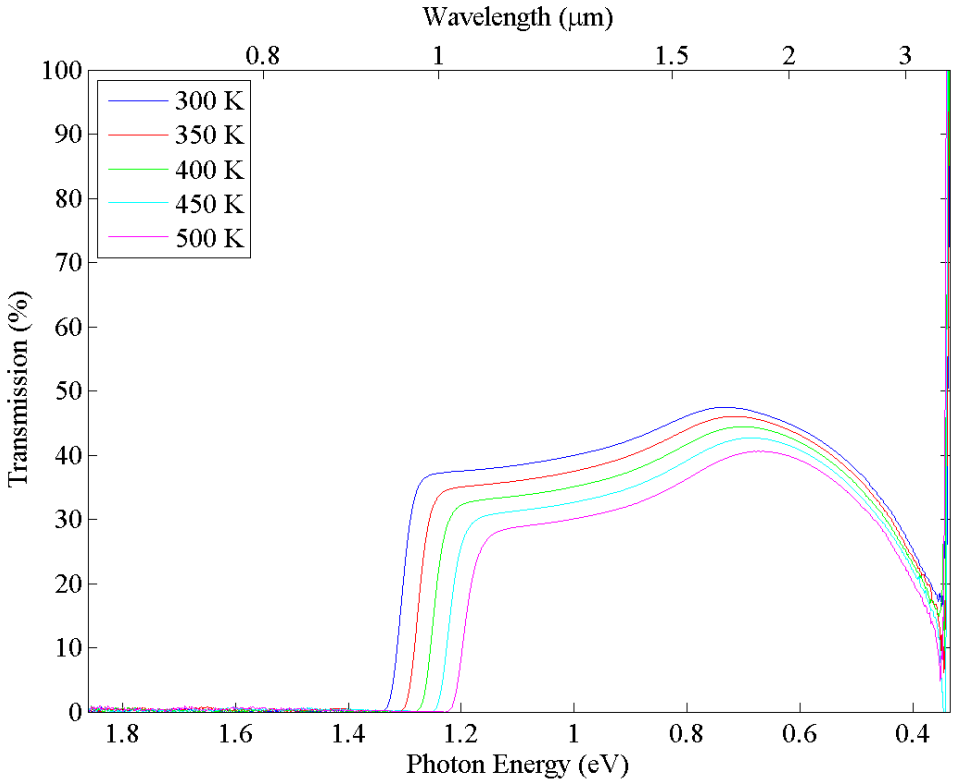

Figure 32. Near infrared transmission spectra for InP from 300 to 500 K

The band gap shift is visible and the absorption edge does not change shape much as temperature increases. There is actually an increase in transmission from 1 to ~1.7 microns which is most likely due to ionized impurity scattering. The drop in transmission starting a little before 2 microns, however, does not appear to be due to free carriers since the temperature dependence is very weak. It may be a high-energy tail of the phonon absorption region.

The band gap was calculated as described earlier. The temperature dependence of the observed band gap is plotted in Figure 33 along with 3 curves representing previous work on InP.

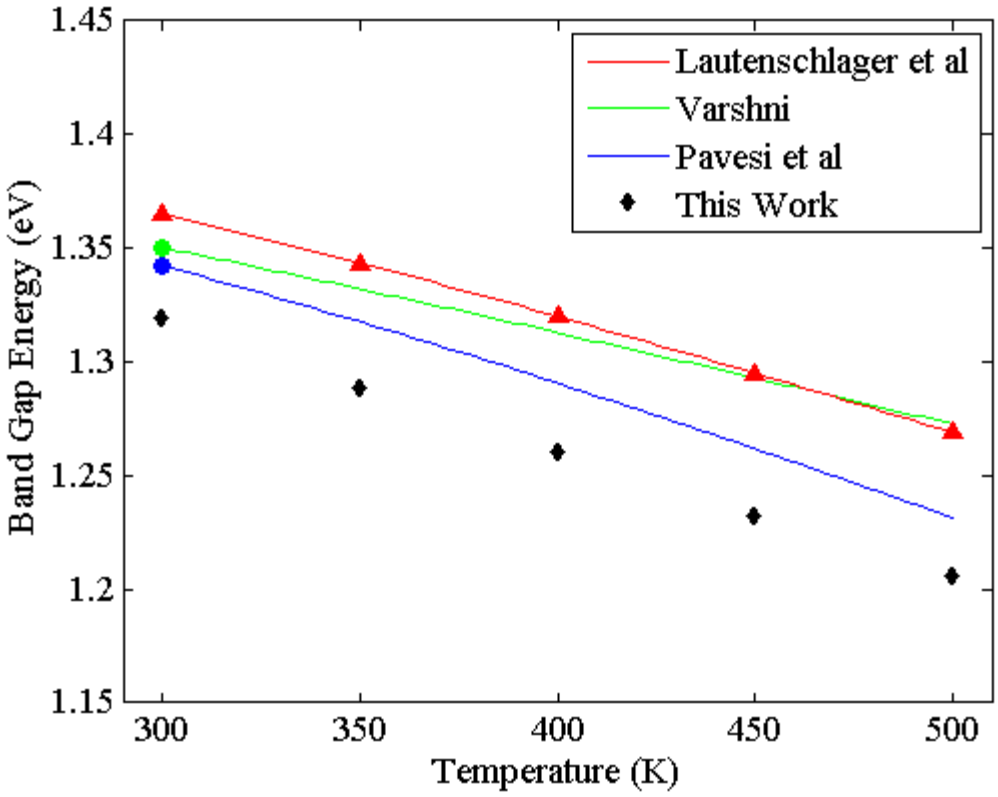

Figure 33. Band gap energy versus temperature for InP from 300 to 500 K

Varshni, shown in green, used the band gap data of Turner et. al. [13] who used low to room temperature photoluminescence to measure the exciton energy, and then calculated the band gap from those values. Lautenschlager et. al. [14], shown in red, used spectroscopic ellipsometry to measure the direct band gap as well as other transitions from 77 to 870 K. More recently Pavesi et. al. [15], shown in blue, measured the band gap of InP from low to room temperature. The results of this work are shown as black diamonds. Again, there is a large difference in the band gap energies compared to the

expected values. The trend seems to match the work of Pavesi et. al. [15] best, although that band gap expression is really being extrapolated since their data only went up to room temperature.

Results for Indium Arsenide (InAs RF4a_2)

Temperature dependent transmission measurements for an undoped InAs sample were taken up to 500 K. The mid-wave infrared transmission is shown in Figure 34. The sample was completely absorbing at about 550 K.

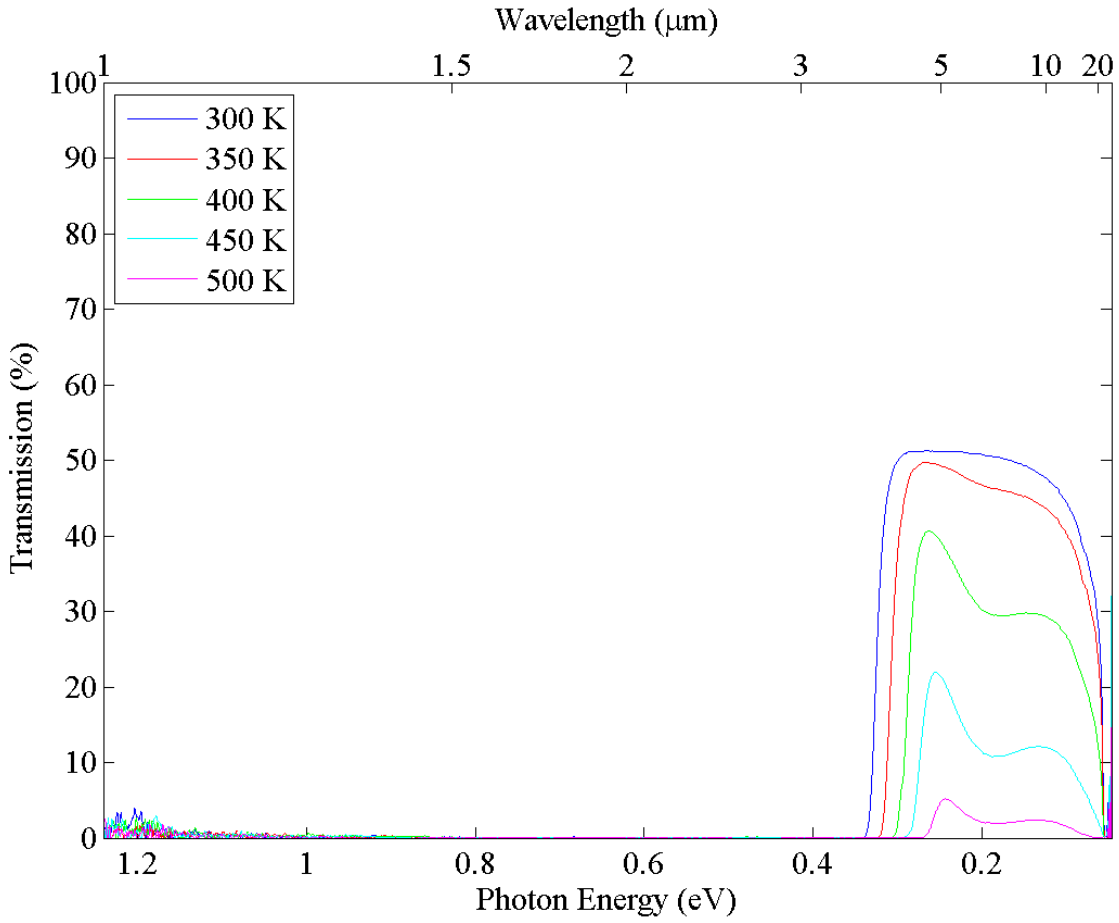

Figure 34. Mid-wave infrared transmission for undoped InAs from 300 to 500 K

The band gap shift is apparent, however, the shape of the transmission curves at the absorption edge begins to change fairly quickly as temperature increases. The band gap was calculated as a function of temperature and the results are plotted along with results from previous work in Figure 35.

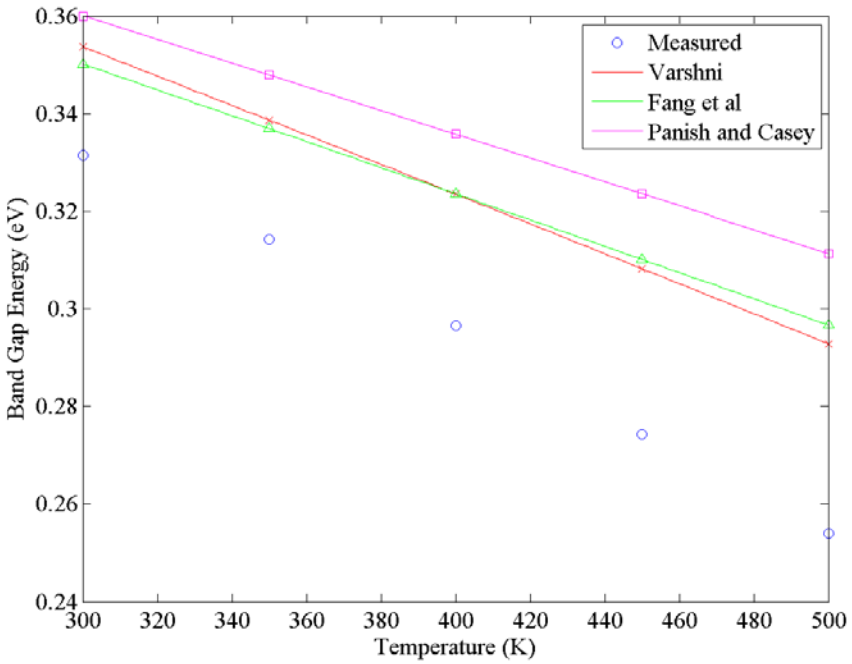

Figure 35. Temperature dependence of the band gap for InAs from 300 to 500 K

Varshni, shown in red, used the band gap data of Dixon and Ellis [16] who used low to room temperature transmission measurements to find the band gap. Fang et. al. [17], shown in green, and Panish and Casey [18], shown in magenta, are fits of their respective band gap data to Vina's equation involving the phonon occupation factor. The results of this work are shown as blue circles. Again, there is a large difference in the band gap energies compared to the expected values. The trend seems to match the work of Dixon and Ellis [16] (fit by Varshni) the best, although again that band gap expression is really being extrapolated since their data only went up to room temperature.

Summary

The measured band gap shift shows good agreement with the theory except for a slight offset. The slopes of the curves are very close. This could have arisen from several factors. An offset that is constant over all temperatures could be a bias error from the spectrometer. This should not be the case, however since the spectrometer was calibrated for each sample. A background scan was done without the sample, and then a transmission scan, again without the sample, which yielded 100% transmission across all wavelengths. This should have eliminated any error in the spectrometer data. The other explanation is that the error is from the band gap calculation. This is probably more likely than the first.

However, the analysis of the bang gap calculation shown in the above figures seems to indicate good extrapolations that are very close to the absorption curve in the linear range. Of course, the “linear range” of the observed absorption curve may not be representative of the actual absorption edge. This again goes back to the fact that there is a maximum absorption that could be measured for the given material type and sample thickness. If the slope of the measured absorption curve differed significantly from the slope at higher absorption levels, then the band gap calculations would be off in energy. Unfortunately, it is impossible to determine if the theory just mentioned was the actual cause of the error in the band gap values. Also, because the upper limit to the measured absorption is intrinsic to the method of the transmission measurements, another method would have to be used in order to measure the higher absorption levels above the onset of absorption edge.

IV. Conclusions and Recommendations

Conclusions of Research

Temperature dependent transmission measurements were carried out for Si, Ge, GaAs, GaSb, InAs, and InP from 0.6 to 25 μm at temperatures ranging from 295 up to 900 K. Band gap shifts were observed as temperature changed and were compared to previous work. General agreement was seen in the trend of the change in the band gap with temperature, however, the actual band gap energy values deviated from the expected on average by about 10%.

Other absorption features were observed such as free carrier absorption, ionized impurity scattering, and multiphonon absorption. The free carrier absorption fit the expected λ^2 dependence well for most material. In the case of Si, this was used to calculate the temperature dependence of the carrier concentration. Multiphonon effects in Si and Ge were shown to match well with previous work.

In general, the absorption was observed to increase dramatically at higher temperatures, specifically above 500 K. This is an expected result, but nonetheless interesting. For the given sample thicknesses, it can be seen that the linear absorption can be very substantial at only moderately high temperatures. 500 K may be higher than the usual temperatures experienced by a device in operation, but there are many applications in which this temperature could easily be reached.

One such application would be laser heating, in which case the time required to heat a sample to about 500 K or even higher could be very short. For example in nonlinear optical measurements, it seems linear absorption due to laser heating could be a factor that would need to be taken into account. This would depend highly on the

situation at hand and the relevant parameters, i.e. laser power, sample type, sample thickness, relative sample impurity (doping), etc.

Recommendations for Future Research

Transmission measurements could be done up to higher temperatures if the apparatus could be contained in a dewar and the sample chamber put under high vacuum. This would reduce oxidation for all samples as well as dissociation for the binary materials. Also for some samples, say GaAs or InP, either As or P gas could be pumped into the chamber to further reduce dissociation and subsequent surface damage. Also, to reduce the number of unknowns in the resulting calculations, reflectance measurements could be made in tandem with the transmission measurements.

Another possibility for future work would be to study the high temperature behavior of other materials. Other binary compounds such as GaP, InSb, etc., are possibilities as are bulk materials with coatings or thin films, or ternary alloys. To further understand and/or verify the free carrier absorption results, temperature dependent Hall Effect measurements could be carried out to determine the carrier concentration as a function of temperature. Also, resistivity measurements taken at room temperature could give an estimate of carrier, and therefore doping concentrations.

Bibliography

1. C. Kittel. *Introduction to Solid State Physics*, 5th edition. J. Wiley & Sons, New York, 1976.

2. N. W. Ashcroft, D. N. Mermin, *Solid State Physics*, 1st edition. Thomson Learning, Toronto, 1976

3. Varshni, V. P., "Band-to-Band Radiative Recombination in Groups IV, VI, and III-V Semiconductors" *Physica Status Solidi*, 19: 459-514 (1967).

4. L. Vina et. al., "Temperature Dependence of the Dielectric Function of Germanium" *Physical Review B*, 30: 1979-1991 (1984).

5. D. K. Schroder, *Semiconductor Material and Device Characterization*, 2nd edition. Wiley, 1998.

6. G. G. Macfarlane et. al., "Fine Structure in the Absorption-Edge Spectrum of Silicon" *Physical Review*, 111: 1245-54 (1958).

7. http://www.ioffe.ru/SVA/NSM/Semicond/Si/optic.html

8. *Handbook Series on Semiconductor Parameters* (volume 1). Ed. Levenshtein M., S. Rumyantsev, and M. Shur. World Scientific, New York, 1996.

9. D. K. Schroder et. al., "Free Carrier Absorption in Silicon" *IEEE Transactions on Electron Devices*, 25: 254-261 (1978).

10. R. J. Collins and H. Y. Fan, "Infrared Lattice Absorption Bands in Germanium, Silicon, and Diamond" *Physical Review*, 93: [10].

11. Macfarlane et. al., "Fine Structure in the Absorption-Edge Spectrum of Germanium" *Physical Review*, 108: 1377-1383 (1957).

12. M.-C. Wu and C.-C. Chen, "Photoluminescence of high-quality GaSb grown from Ga- and Sb-rich solutions by liquid-phase epitaxy" *Journal of Applied Physics*, 72: 4275-4280 (1992).

13. W. J. Turner et. al., "Exciton Absorption and Emmission in InP" *Physical Review*, 136: A1467-1470 (1964).

14. P. Lautenschlager et. al., “Temperature dependence of the interband critical-point parameters of InP” *Physical Review B*, 36: 4813-4820 (1987).

15. L. Pavesi and F. Piazza, “Temperature dependence of the InP band gap from a photoluminescence study” *Physical Review B*, 44: 9052-9055 (1991).

16. Jack R. Dixon and James M. Ellis, “Optical Properties of *n*-Type Indium Arsenide in the Fundamental Absorption Edge Region” *Physical Review*, 123: 1560-1566 (1961).

17. Z. M. Fang et. al., “Photoluminescence of InSb, InAs, and InAsSb grown by organometallic vapor phase epitaxy” *Journal of Applied Physics*, 67: 7034-7040 (1990).

18. H. C. Casey, Jr. and M. B. Panish, *Heterostructure Lasers* Vol. 2, pp. 9-10, Academic, New York, 1978.

REPORT DOCUMENTATION PAGE

Form Approved
OMB No. 074-0188

1. REPORT DATE *(DD-MM-YYYY)*	2. REPORT TYPE	3. DATES COVERED *(From – To)*
25-03-2010	Master's Thesis	March 2009 – March 2010

4. TITLE AND SUBTITLE

Optical Properties of Si, Ge, GaAs, GaSb, InAs, and InP at Elevated Temperatures

5a. CONTRACT NUMBER

5b. GRANT NUMBER

5c. PROGRAM ELEMENT NUMBER

6. AUTHOR(S)

Harris, Thomas R., DAGSI

5d. PROJECT NUMBER
If funded, enter ENR #

5e. TASK NUMBER

5f. WORK UNIT NUMBER

7. PERFORMING ORGANIZATION NAMES(S) AND ADDRESS(S)
Air Force Institute of Technology
Graduate School of Engineering and Management (AFIT/EN)
2950 Hobson Way, Building 640
WPAFB OH 45433-8865

8. PERFORMING ORGANIZATION REPORT NUMBER

AFIT/GAP/ENP/10-M08

9. SPONSORING/MONITORING AGENCY NAME(S) AND ADDRESS(ES)
Dr. Shekhar Guha
Air Force Research Laboratory
Materials and Manufacturing Directorate
WPAFB, OH 45433

10. SPONSOR/MONITOR'S ACRONYM(S)
AFRL/RXP

11. SPONSOR/MONITOR'S REPORT NUMBER(S)

12. DISTRIBUTION/AVAILABILITY STATEMENT

APPROVED FOR PUBLIC RELEASE; DISTRIBUTION UNLIMITED.

13. SUPPLEMENTARY NOTES

14. ABSTRACT

Investigation of the optical and electrical behavior of some semiconductors at very high temperatures has not been an area of much study, at least not experimentally. The importance of such research becomes obvious due to the effects of high temperatures on semiconductor devices such as infrared detectors and light emitters. Besides the destructive effects of thermal stress and melting, changes in the optical properties of the material can greatly affect device performance. In this research, the infrared absorption of Si, Ge, GaAs, GaSb, InAs, and InP was measured from 0.6 to 25 μm at temperatures ranging from 295 up to 900 K, using a Fourier Transform InfraRed (FTIR) spectrometer in combination with a custom-designed heater assembly. The band gap shift was estimated from the experimental results and compared to existing data. There was good agreement between the two results. For GaSb and InAs, data was taken at higher temperatures than what was found in the literature. That data provides an extension of existing theory to a higher temperature range. Free-carrier absorption was also observed and was compared to existing data. Temperature dependent expressions were developed for the band gap energy and free-carrier absorption in Si, Ge, GaAs, GaSb, InAs, and InP.

15. SUBJECT TERMS

16. SECURITY CLASSIFICATION OF:			17. LIMITATION OF ABSTRACT	18. NUMBER OF PAGES	19a. NAME OF RESPONSIBLE PERSON
a. REPORT	b. ABSTRACT	c. THIS PAGE			Dr. Yung Kee Yeo, ENP
U	U	U	UU	74	19b. TELEPHONE NUMBER *(Include area code)* (937) 255-3636, x4532; email: yung.yeo@afit.edu

Standard Form 298 (Rev. 8-98)
Prescribed by ANSI Std. Z39-18